PERMEABILITY ESTIMATION FROM VELOCITY ANISOTROPY IN FRACTURED ROCK

by

Richard L. Gibson, Jr. and M. Nafi Toksöz

Earth Resources Laboratory
Department of Earth, Atmospheric, and Planetary Sciences
Massachusetts Institute of Technology
Cambridge, MA 02139

ABSTRACT

Cracks in a rock mass subjected to a uniaxial stress will be preferentially closed depending on the angle between the fracture normal vectors and the direction of the applied stress. If the prestress fracture orientation distribution is isotropic, the effective elastic properties of such a material after application of the stress are then transversely isotropic due to the overall alignment of the cracks still open. Velocity measurements in multiple directions are used to invert for the probability density function describing orientations of crack normals in such a rock. This is accomplished by expanding the crack orientation distribution function into generalized spherical harmonics. The coefficients in this expansion are functions of the crack density and the crack aspect ratio distribution. The information on fracture distribution obtained from the velocity inversion allows an estimation of the anisotropic permeability of the fractured rock system. Permeability estimates are based on the number of cracks open of each aspect ratio, and the contribution of a given crack is weighted by the cosine of the angle between the crack and the direction of the applied pressure gradient. This approach yields a prediction of permeability as a function of the angle from the uniaxial stress axis. The inversion for crack orientation is applied to ultrasonic velocity measurements on Barre granite, and permeability predictions for this sample are presented. The inversion results are good and reproduce velocity measurements well, and the permeability predictions show some of the expected trends. Initial comparisons of the predictions with available permeability data, however, show deviations suggesting that further information on partial crack closure and connectivity of cracks should be included in the permeability model.

INTRODUCTION

A common goal of seismic field experiments is to estimate rock properties such as permeability from the information contained in the seismic waveforms. Fractured media provide a particularly interesting example of a permeable medium, since a material containing an aligned system of cracks will be effectively anisotropic for elastic wavelengths much greater than the crack dimensions (Hudson, 1980, 1981; Crampin, 1984). While a particular rock may have a randomly oriented distribution of cracks, application of a uniaxial stress will preferentially close fractures depending on orientation with respect to the stress axis (Walsh, 1965; Nur, 1971). It has been suggested that the prevailing tectonic stress regimes in the earth frequently include a maximum compressive stress which is horizontal, resulting in such an alignment of vertically oriented cracks (Crampin, 1981). A uniaxial stress is easily produced in laboratory experiments as well (Nur and Simmons, 1969).

Analysis of the elastic anisotropy produced by crack alignment can be used to investigate fracture properties. Sayers (1988a,b) suggested a means of inverting for the orientations of crack normals using these velocity measurements. This method involves an expansion of the fracture orientation distribution function in terms of harmonics related to the system of Euler angles describing the orientations. The coefficients in the expansion are subsequently related to perturbations in elastic moduli predicted by the Hudson (1981) theory for the properties of a cracked medium, and an inversion was performed based on an approximate expression for elastic wave velocity derived from a variational approach (Sayers, 1988a,b).

In this paper, we apply an alternative form of an inversion for crack orientations. A nonlinear inversion is performed by linearizing the phase velocity expressions about an initial estimate of crack density and a parameter describing the distribution of crack aspect ratios. The resulting estimate of crack orientations and the distribution of aspect ratios with respect to direction is used to predict permeability as a function of direction with respect to the uniaxial stress axis. These permeability predictions are calculated based on a model for permeability in the fractured medium which accounts for crack closure effects by multiplication by the fraction of cracks open in a given direction. The method is applied to ultrasonic velocity data for Barre granite (Nur and Simmons, 1969) and the implications of the results for permeability prediction are discussed.

THEORY

Inversion for crack orientations

The rock medium is assumed to contain an isotropic distribution of cracks in the unstressed state so that the effective elastic parameters of the material are also isotropic in this case. When a uniaxial stress is applied to such a material, some of the cracks will close depending on the angle of the crack normal with respect to the stress axis (Walsh, 1965) (Figure 1). This angle γ_0 is given by

$$\cos \gamma_0 = \sqrt{\frac{\alpha E_0}{\sigma}}, \tag{1}$$

where α is the crack aspect ratio, E_0 is the Young's modulus of the uncracked material, and σ is the applied uniaxial stress. The initially isotropic material will become anisotropic after application of the stress with rotational symmetry about the stress axis (Nur, 1971). The effective elastic properties of the stressed, cracked material will then have a transversely isotropic symmetry.

The effective elastic moduli of the medium can be estimated by averaging the elastic constants of the fractured material over a crack orientation distribution function $N(\theta, \psi, \phi)$, where θ, ψ, and ϕ are Euler angles of rotation specified in Figure 2. These angles define the set of rotations necessary to obtain the orientation of the crack Cartesian coordinate system x, y, z for each crack with respect to the composite medium reference Cartesian coordinate system denoted by X, Y, Z. We specify the initial orientation of the fracture prior to rotation such that the crack normal (parallel to z) is parallel to Z, and the other two axes x and y are therefore in the plane of the fracture. Note that for a circular crack, only θ and ψ are necessary to fully specify crack orientations, and ϕ can freely range from 0 to 2π. The crack orientation distribution function $N(\theta, \psi, \phi)$ is defined so that integration over the full domain is one:

$$\int_0^{2\pi} \int_0^{2\pi} \int_0^{\pi} N(\theta, \psi, \phi) \, d\theta \, d\psi \, d\phi = 1. \tag{2}$$

This function can be expanded in generalized spherical harmonics

$$N(\theta, \psi, \phi) = \sum_{l=0}^{\infty} \sum_{m=-l}^{l} \sum_{n=-l}^{l} W_{lmn} Z_{lmn}(\zeta) e^{-im\psi} e^{-in\phi}. \tag{3}$$

Here $\zeta = \cos \theta$. The derivation of the generalized Legendre functions $Z_{lmn}(\zeta)$ and some of their properties are described by Ben-Menahem and Singh (1981). Each coefficient W_{lmn} in the expansion of the orientation distribution function $N(\zeta, \psi, \phi)$ is obtained by integrations of the following form:

$$W_{lmn} = \frac{1}{4\pi^2} \int_0^{2\pi} \int_0^{2\pi} \int_{-1}^{1} N(\zeta, \psi, \phi) Z_{lmn}(\zeta) e^{im\psi} e^{in\phi} \, d\zeta \, d\psi \, d\phi. \tag{4}$$

With this expansion, the orientation distribution function can be decomposed into harmonic components.

If a polycrystalline aggregate were considered, an estimate of the elastic properties of the aggregate could be obtained by simply averaging the elastic constants of the individual crystals with respect to the orientation distribution. This method, the Voigt approach, is known to yield an upper bound on the elastic constants (Hearmon, 1961). The same procedure can be applied to the fractured medium by averaging the effective elastic constants of fractured material over all sets of fracture orientations in the rock (Sayers, 1988a). Since this is an upper bound, and it is not clear how far removed from the true solution this bound is, there will be some limitations on the accuracy of the results which is not well defined. Application of similar techniques to other problems involving cracks has shown that resulting errors are generally not too large for smaller crack concentrations, however (Walsh, 1965). The averaged constants can be written (Morris, 1969)

$$\overline{c}_{ijkl} = c_{mnpq} \int_0^{2\pi} \int_0^{2\pi} \int_{-1}^{1} T_{ijklmnpq}(\zeta, \psi, \phi)\, N(\theta, \psi, \phi)\, d\zeta\, d\psi\, d\phi \qquad (5)$$

$$= c_{mnpq} \overline{T}_{ijklmnpq}$$

$$T_{ijklmnpq} = \frac{\partial x_i}{\partial X_m} \frac{\partial x_j}{\partial X_n} \frac{\partial x_k}{\partial X_p} \frac{\partial x_l}{\partial X_q}.$$

The Einstein summation convention is applied. The matrix $\overline{T}_{ijklmnpq}$ essentially defines an average rotation of the elastic constants of the individual components c_{mnpq}, which for the polycrystalline case are the elastic constants of a single crystal and for the fractured material case are the constants corresponding to a single set of parallel fractures. Morris (1969) has calculated a table of values for the matrix elements $\overline{T}_{ijklmnpq}$ in terms of the coefficients of the expansion of the distribution function up to order $l = m = n = 4$ for composites of materials with orthorhombic symmetry which can also be applied to material with hexagonal symmetry. The orthogonality properties of the harmonics cause terms for indices greater than 4 to disappear since the fourth order elastic tensor c_{mnpq} will only have coefficients for $l = m = n = 4$. The Morris (1969) table can easily be used in Eq. (5) to find the overall properties.

The theory of Hudson (1980, 1981) for the stiffness constants of a fractured medium can be used to obtain values for c_{ijkl} to use on the right hand side of Eq. (5). This theory provides an expression for the effective elastic tensor c_{ijkl} of a homogeneous medium containing a single set of parallel penny shaped cracks with dimensions much less than a wavelength. This expression is in terms of a first order correction c_{ijkl}^1 to the elastic tensor of the unfractured material c_{ijkl}^0:

$$c_{ijkl} = c_{ijkl}^0 + \epsilon\, c_{ijkl}^1. \qquad (6)$$

Here ϵ is the crack density defined by $\epsilon = n\alpha^3$, n is the number of cracks per unit volume, and a is the crack radius. Hudson (1980) also derived a second order term which results

in values of the stiffnesses which are quadratic functions of the concentration of cracks, and hence the second order theory actually displays divergent behavior for large crack concentrations. In order to match the observed data discussed below, the second order correction was therefore not applied.

If we apply a stress along the z-axis, the only nonzero coefficients in the expansion of the resulting crack distribution will be W_{000}, W_{200}, and W_{400} due to the symmetry around the z-axis and the circular symmetry of the cracks. For purposes of the inversion, we follow Nur (1971) and Sayers (1988b) and take as a model for the crack aspect ratio distribution in the unstressed state a simple linear function

$$N^l(\alpha) = N_0^l(1 - \frac{\alpha}{\alpha_m}), \qquad 0 < \alpha < \alpha_m. \tag{7a}$$

The parameter α_m sets the maximum aspect ratio present in the rock sample and is given by $\alpha_m = \sigma_0/E_0$, where σ_0 is the hydrostatic pressure required to close all cracks. To serve as a density function Eq. (7a) is normalized by the total number of cracks present n_σ^l at stress σ:

$$n_\sigma^l = N_0^l \left[\frac{\alpha_m}{2} + \frac{\sigma^2}{E_0^2} \frac{1}{10\alpha_m} - \frac{\sigma}{3E_0} \right] \tag{8a}$$

Given this distribution of cracks, the crack orientation distribution function after application of a uniaxial stress can be obtained using the closure model given by Eq. (1). At any given angle θ from the stress axis, all fractures with aspect ratio $\alpha > \sigma \cos^2 \theta / E_0$ are open. The resulting coefficients in the expansion of the orientation distribution function are:

$$W_{000} = \frac{1}{8\pi^2},$$

$$W_{200} = -\frac{1}{5n_\sigma^{ll}2\pi^2}\sqrt{\frac{5}{2}}\frac{\sigma}{E_0}\left(\frac{1}{3} + \frac{1}{7}\frac{\sigma}{E_0\alpha_m}\right),$$

$$W_{400} = \frac{1}{315}\frac{1}{n_\sigma^{ll}\pi^2}\sqrt{\frac{9}{2}}\frac{\sigma^2}{E_0^2\alpha_m},$$

$$n_\sigma^{ll} = \frac{n_\sigma^l}{N_0^l}. \tag{9a}$$

One important aspect of this particular distribution model is that the expansion up to terms $l = 4$ is exact, and there is therefore no truncation error from termination of the series. If, however, only a single crack aspect ratio were considered, the post-stress distribution of cracks resulting from the closure model governed by Eq. (1) would be a box car function with respect to the θ (or η) variable, and strong Gibbs phenomena effects would result since accurate representation of this discontinuous function will require a large number of terms in the expansion. Truncation of the expansion series

in this case would yield unrealistic results due to strong oscillations of the predicted distribution function.

The choice of aspect ratio in Eq. (7a) is rather arbitrary and may not be truly representative of the cracks within a rock sample, though accuracy of results using the distribution will give some indication of its validity. For purposes of comparison in applications, we also consider a flat aspect ratio distribution

$$N^f(\alpha) = N_0^f, \qquad 0 < \alpha < \alpha_m \ . \tag{7b}$$

For this aspect ratio distribution, the normalization constant is

$$n_\sigma^f = N_0^f \left[\alpha_m - \frac{1}{3} \frac{\sigma}{E_0} \right] , \tag{8b}$$

and the coefficients in the generalized spherical harmonic representation are

$$
\begin{aligned}
W_{000} &= \frac{1}{8\pi^2}, \\
W_{200} &= -\frac{1}{n_\sigma^{f\prime} 30\pi^2} \sqrt{\frac{5}{2}} \frac{\sigma}{E_0}, \\
W_{400} &= 0, \\
n_\sigma^{f\prime} &= \frac{n_\sigma^f}{N_0^f}.
\end{aligned}
\tag{9b}
$$

The results for this hypothetical distribution of cracks may be compared to those obtained using the distribution given in Eq. (7a).

Given the values of the elastic constants resulting from the averaging process, velocities can be computed for the stressed, cracked material. The quasi-compressional wave phase velocity v_{qP}, vertically polarized quasi-shear wave velocity v_{qSV}, and horizontally polarized shear wave velocity v_{SH} in a general transversely isotropic medium are given by (Musgrave, 1970)

$$\rho v_{qP}^2 = \overline{C}_{44} + \frac{1}{2} \left\{ h\cos^2\beta + a\sin^2\beta + \left[(h\cos^2\beta + a\sin^2\beta)^2 - 4(ah - d^2)\cos^2\beta\sin^2\beta \right]^{1/2} \right\} \tag{10}$$

$$\rho v_{qSV}^2 = \overline{C}_{44} + \frac{1}{2} \left\{ h\cos^2\beta + a\sin^2\beta - \left[(h\cos^2\beta + a\sin^2\beta)^2 - 4(ah - d^2)\cos^2\beta\sin^2\beta \right]^{1/2} \right\} \tag{11}$$

$$\rho v_{SH}^2 = \overline{C}_{44}\cos^2\beta + \overline{C}_{66}\sin^2\beta \tag{12}$$

$$
\begin{aligned}
a &= \overline{C}_{11} - \overline{C}_{44} \\
h &= \overline{C}_{33} - \overline{C}_{44} \\
d &= \overline{C}_{13} + \overline{C}_{44}.
\end{aligned}
$$

Here β is the angle measured from the symmetry axis, in this case the z-axis, and the standard 6 by 6 form for the tensor of elastic constants has been utilized. This expression uses the averaged elastic constants to predict the phase velocity value in a given direction.

For a given uniaxial stress σ and intrinsic Young's modulus E_0, the only unknown parameters necessary to compute velocity from Eq. (10) are crack density ϵ and maximum crack size α_m. Therefore, these are the natural quantities to determine through inversion procedures. Since Eq. (10) is a nonlinear function of ϵ and α_m (through the dependence of the elastic constants on the orientation function), an inversion is performed by linearizing the problem about an initial estimate of model parameters (Tarantola, 1987; Hatton et al., 1986):

$$d \cong Gm_0 + A\Delta m. \tag{13}$$

Here d is the data vector containing observed velocity values, G is the forward model operator yielding velocity predictions for a given set of model parameters in starting model vector m_0, A is a matrix of partial derivatives of velocity with respect to model parameters, and Δm is a perturbation to the starting estimate of model values. The partial derivatives are somewhat complicated algebraically, but can be computed analytically with no approximations. We then perform an iterative least squares inversion for the model parameters α_m and ϵ, which allows an estimate of the crack normal orientation distribution.

The forward modeling part of this inversion procedure is similar to that proposed by Sayers (1988a,b), but there are several significant differences. For example, Sayers (1988b) considers a stress applied along the x-axis, which results in a more complicated expansion of the crack orientation distribution function since the orientation is in that case a function of angle ψ as well as θ. The approach described in this paper uses the exact expression for phase velocity, while Sayers (1988b, see also 1986) uses an approximate expression derived from a variational method.

More important than these considerations, however, are the differences in inversion algorithms. Sayers (1988b) proposes what is essentially a curve fitting methodology where v_{qSV} is approximated by a constant and v_{qP} and v_{SH} are approximated as the sum of a constant and a $\cos 2\theta$ term. The coefficients of these functions are then determined using a least squares procedure, and crack density is obtained from the values of the coefficients. Since there are at most two coefficients in any one of the velocity expressions, only two parameter values can be obtained in this way, though Sayers (1988b) chooses only to attempt to estimate crack density ϵ. In contrast, the procedure suggested here uses the complete expressions for the velocities and for the partial derivatives in the inversion. As many parameters as there are data points can be estimated by this approach, and data types from different experiments can easily be combined in a single inversion. For example, velocity measurements from different stress values can be used to invert for crack density at each stress and for a single value of α_m, which

should remain constant for a given rock sample. On the other hand, the curve fitting approach will only allow a determination of the coefficients for each data curve at each stress, and does not truly allow a combination of the data sets.

Perhaps the most important advantage of the more complex inversion scheme in seeking to understand the properties of the physical model and of the effects of the cracks on the propagation of elastic waves is that consideration of the partial derivatives allows insights into the sensitivity of the inversion to each of the various parameters. In turn, this gives more information on the validity of inversion results and on the factors which are important in controlling velocity variations within the fractured medium. A disadvantage of this more complicated inversion algorithm is that it is potentially more susceptible to problems such as nonuniqueness and local minima, whereas the curve fitting approach will tend to be more robust.

Permeability prediction

The crack orientation distribution function resulting from the inversion can be used to predict permeability values. The permeability of a single fracture of aperture L_0 is simply

$$k_1 = \frac{L_0^3}{12}. \tag{14}$$

This cubic law permeability results from the analysis of flow through a single parallel plane walled fracture (Snow, 1969), and gives the flow rate per unit length along the fracture. Conventional permeability values are defined from Darcy's law relative to flow across a unit surface element area. To make this conversion, consider as a model a block volume containing a set of cracks which extend through the length of the block. The permeability of the volume relative to the surface area of the block is obtained by simply adding the contribution of each fracture, which amounts to multiplying Eq. (14) by the number of cracks in the volume. The number of cracks of interest is the number with normals perpendicular to the direction in which permeability is to be estimated, which requires a knowledge of the crack normal distribution function $P^l(\chi, \eta)$, $\chi = \cos\delta$ (Figure 3). The superscript l refers to the linear aspect ratio distribution in Eq. (7a) and a superscript f would refer to the flat distribution. Due to the circular symmetry of the cracks, this function is equal to $2\pi N^l(\zeta, \psi, \phi)$ so that $\chi = \zeta$ and $\eta = \psi$. Remembering that $\epsilon = na^3$, a set of cracks of density ϵ_0 with aspect ratio α yields a permeability k_α

$$k_\alpha = \frac{\epsilon_0 \alpha^3}{12}, \tag{15}$$

where the product in the numerator gives nL_0^3. Since the model considers a unit volume, the dimensions of k_α in Eq. (15) are length squared, where the length unit will be the same as that of the unit volume under consideration.

Integrating over the range of crack aspect ratios for cracks still open in a given direction, from $\alpha_{cl} = \cos^2 \gamma_0 \sigma / E_0$ to α_m, using the linear aspect ratio distribution from Eq. (7a) gives permeability as a function of angle θ measured from the stress axis for all of the cracks in this direction:

$$k'(\theta - \pi/2) = \frac{\epsilon}{96\pi^2 \left(\frac{\alpha_m^2}{2} \frac{\sigma^2}{E_0^2} \frac{1}{10} - \frac{\alpha_m}{3} \frac{\sigma}{E_0} \right)} \left[\frac{\alpha_m^5}{20} - \frac{\alpha_m}{4} \frac{\sigma^4}{E_0^4} \cos^8 \theta + \frac{1}{5} \frac{\sigma^5}{E_0^5} \cos^{10} \theta \right] . \quad (16)$$

Cracks oriented in directions other than parallel to the applied pressure gradient will also have a contribution to the permeability. The effects of these cracks can be partially included by adding their permeability, multiplied by the cosine of the angle between each fracture set and the direction of the pressure gradient. Restricting attention to crack normals within a single vertical plane, such as the $x - z$ plane, we can integrate the result of Eq. (16) multiplied by the appropriate cosine function:

$$\int_{\gamma - \frac{\pi}{2}}^{\gamma + \frac{\pi}{2}} k'(\theta - \pi/2) \cos(\gamma - \theta) d\theta . \quad (17)$$

Here $\gamma - \pi/2$ is the direction of interest for the permeability estimation. In principle, cracks with normals outside of the vertical plane could be considered, but it turns out that the resulting integral is very complicated and does not add significant insight to the resulting permeability model. Carrying out the integration in Eq. (17), we have for the linear aspect ratio distribution

$$k^l(\gamma - \pi/2) = \frac{\epsilon}{48\pi^2 \left(\frac{\alpha_m^2}{2} \frac{\sigma^2}{E_0^2} \frac{1}{10} - \frac{\alpha_m}{3} \frac{\sigma}{E_0} \right)} X^l , \quad (18)$$

$$X^l = \frac{\alpha_m^5}{20} - \frac{\alpha_m}{4} \frac{\sigma^4}{E_0^4} \frac{1}{9} \left[\frac{\cos^2}{35} \left(128 + 128 \sin^2 \gamma + 48 \sin^4 \gamma + 40 \sin^6 \gamma + 35 \sin^6 \gamma \right) + \sin^{10} \gamma \right]$$
$$+ \frac{1}{55} \frac{\sigma^5}{E_0^5} \left[\frac{\cos^2 \gamma}{63} \left(256 + 256 \sin^2 \gamma + 96 \sin^4 \gamma + 80 \sin^6 \gamma + 70 \sin^8 \gamma + 63 \sin^{10} \gamma \right) + \sin^{12} \gamma \right] .$$

The same procedure can be performed for the flat aspect ratio case (Eq. (7b)), and the resulting permeability expression is

$$k^f(\gamma - \pi/2) = \frac{\epsilon}{192\pi^2} \frac{1}{\alpha_m - \frac{1}{3} \frac{\sigma}{E_0}} X^f , \quad (19)$$

$$X^f = \alpha_m^4 - \frac{\sigma^4}{E_0^4} \frac{1}{9} \left[\frac{\cos^2}{35} \left(128 + 128 \sin^2 \gamma + 48 \sin^4 \gamma + 40 \sin^6 \gamma + 35 \sin^6 \gamma \right) + \sin^{10} \gamma \right] .$$

These two results may be used to provide an estimate to permeability within the fractured rock as uniaxial stress is applied. If the uniaxial stress is sufficiently large to close

off all cracks present in a given direction, then the integration limits in Eq. (17) must be changed to account for the range of angles where no cracks are present. This results in expressions very similar to the permeability results in Eqs. (18) and (19).

While this appears to be a simple approach to permeability estimation, it is related to other studies of fluid flow through crystalline rock. Bernabé (1986) examines in detail the applicability of the equivalent channel concept to permeability modeling for several granites and concludes that it is a valid approach. Our case is analogous to an equivalent channel model in that we replace the complicated fracture network by a simplified representation of sets of plane walled fractures extending through the medium, though we do not base our "channel" on some of the conventional concepts of the surface area and volume of the porous structure. However, the model does include the effects of crack closure as a function of direction. Some of the effects which are neglected are the diminished aperture of cracks due to asperities and the complicated flow paths within the rock. The effect of surface roughness of cracks is probably not too important over relatively low pressure ranges, since fractures with asperities still display a cubic law permeability behavior with an effective, mean crack width (Tsang and Witherspoon, 1981, 1983). Numerical studies of fluid flow through cracks with asperities confirm this conclusion (Brown, 1987). Therefore, the tortuosity effect is of much greater concern. The most direct way to include the tortuosity is to simply normalize the permeability predictions by some constant so that the values are of the correct order of magnitude. This can be done easily if permeability for one direction is known or if the permeability of the unstressed rock is known.

It is important that we have only included a fracture contribution to permeability in this model. If the medium under consideration has a significant amount of a different type of interconnected pores and tubular fluid conduits, such as is the case in some sandstones, the effects of the crack closure must be added to the permeability due to other porosity types. Since the equidimensional pores of a sandstone will only be minimally affected by the applied stress, the effects of the cracks may not be so important for overall permeability values. This crack model is most important for low porosity rocks such as fractured limestones or granites and other crystalline and metamorphic rocks which would be essentially impermeable except for the cracks.

The permeability model also essentially assumes a prestress isotropicity of the fracture network creating the permeability of the rock medium. It is conceivable that some particular arrangements of cracks and their intersections might show strong variations in effective permeability depending on the direction of the applied stress, but the model assumes that this effect will not occur and that the behavior of the medium is independent of the direction of the stress axis. Therefore the cracks in the medium must on average have an isotropic distribution in both orientation and in intersection properties.

APPLICATION TO ULTRASONIC DATA

The inversion procedure together with the permeability models Eqs. (18) and (19) provide a method for predicting permeability values given observations of elastic wave velocities which could be obtained from either laboratory samples or field data. Nur and Simmons (1969) made velocity measurements on samples of Barre granite as a function of direction for several magnitudes of applied uniaxial stress. Measurements were presented for both quasi-compressional wave signals and quasi-transverse waves, SV and SH. The Barre granite sample used by Nur and Simmons (1969) was dry, so the Hudson (1981) formulation for dry cracks is appropriate. A value of 2.7 gm/cm^3 was used for density in the equations required for the inversion, and the Lamé parameters used to compute the Young's modulus were $\lambda_0 = 22.05$ GPa and $\mu_0 = 35.97$ GPa (Nur, 1971).

Velocity inversions

Velocity data for qP waves at uniaxial stress values of 0, 10, 20 and 30 MPa were jointly inverted for the crack density ϵ at each stress value and for a single value of maximum aspect ratio α_m. The results for these parameters are given in Table 1 for both the linear and the flat aspect ratio distribution function (Eqs. (7a) and (7b)). Corresponding quasi-compressional wave velocity predictions and observations are compared in Figs. 4 and 5. The theory is able to match the data fairly well, with a fit approximately the same as that obtained by Sayers (1988b). In general, the linear distribution gives a slightly better fit to the observed velocity values. The trends in crack density shown by the inversion results in Table 1 are reasonable. As stress increases, more cracks will close reducing the overall crack density, as occurs for these results. In addition, the two aspect ratio distributions give essentially the same ϵ at each pressure (Table 1). However, the maximum aspect ratio given by the constant distribution function, 3.99×10^{-4}, is about 60% of the value resulting from the linear case, 6.34×10^{-4}. This occurs because with the Walsh (1965) crack closure model, many cracks of small aspect ratio are required to close at low pressures such as 10 or 20 MPa. For example, at 10 MPa, the largest crack which closes, with a normal in the direction of the applied stress, has an aspect ratio of approximately 1.17×10^{-4} for a material with the Lamé parameters used for this inversion. The flat distribution will contain proportionately fewer small aspect ratio cracks for a given total crack density, and so will require a smaller α_m to achieve the same degree of predicted velocity increase for a given applied uniaxial stress.

Analogous results for the SH data are presented in Table 2, and velocity predictions are shown in Figs. 6 and 7. While the SH data are similar to those in Figs. 4 and 5 for the quasi-compressional waves, the qSV results are relatively poor and are given in Table 3 and Figs. 8 and 9. A non-attenuative transversely isotropic medium always has

equal qSV velocities parallel and perpendicular to the symmetry axis (see Eq. (11)), but it is clear from the data in Figure 8 that this condition is not quite true for these observations. It is clear that there is a trend to the qSV velocity with direction that is not reproduced in the variations predicted by the crack model. It is possible that the Barre granite has some slight intrinsic anisotropy which would cause the stressed system to have some overall symmetry other than transversely isotropic. A likely cause of SV velocity variation is preferred grain orientation in the granite. Lo et al. (1986) clearly demonstrate such a residual anisotropy after crack closure in measurements of velocity in Chelmsford granite. If the residual anisotropy is the cause of most of the velocity variation for the SV data, the inversion results are not significant for inference of crack orientation since the forward model involved in the inversion includes only anisotropy due to cracks.

The effects of this residual anisotropy seem to be evident to a smaller degree at high pressures for the quasi-compressional and SH wave data also (Figs. 4, 5, 6 and 7). Since the total velocity anisotropy is greater for the quasi-compressional and SH data, however, the fractures have more effect on observed velocities and the inversion results are more significant for these cases. The values of crack density ϵ obtained from the two quasi-shear wave data sets are very similar, but the quasi-compressional wave data consistently yielded a somewhat lower estimate of crack density. The results for all data sets are also essentially the same as those obtained by Sayers (1988b). In order to examine these differences in estimated crack density, a joint inversion of both SH and qP wave data from experiments at a single uniaxial stress was attempted, but it was found that the value of ϵ obtained was between the values resulting from the individual inversions and predicted velocities too large to match the qP data well, but too small for the SH velocity measurements. The cause of the difference in results for quasi-compressional and quasi-shear wave data is difficult to explain but may be caused by remnant water within the granite sample. Liquid within the cracks would tend to raise the qP wave velocity for a given crack density, while having a much more negligible effect on quasi-shear wave velocities. Therefore, a single value of ϵ would be able to yield velocity predictions matching both sets of data. It would be desirable to repeat the velocity experiment with uniaxial stress taking great care to maintain the dryness of the rock sample in order to confirm this hypothesis.

It is possible that both the qP and SH estimates for crack density are high due to the use of the Voigt approximation in calculating elastic constants (Eq. (5)). Since the Voigt approach gives an upper bound, the averaged constants could be "stiffer" than those of the fractured medium, and a higher density of cracks would then be necessary to reduce the velocities to the observed values. If, however, the qP estimated crack density is reduced by the presence of liquids as suggested above, this will offset the error and the solution will not be too far off. It is likely that the true crack density is near the values we estimate.

Unlike the crack density, the estimates for α_m from qP and SH data are comparable for each aspect ratio distribution. For the flat distribution, the values differ by about 12%, and the variation is about 6% for the linear function. In both cases, the qP inversion yields the smaller estimate for α_m. This difference likely stems from effects similar to those suggested as causing the decrease in crack density estimates.

Although there is some consistency of these inversion results for crack density and for the maximum aspect ratio parameter, it remains to establish the validity of the inversion results and the accuracy of the resulting description of crack geometry within the rock. Several studies involving direct examination of rock samples for crack geometry have been conducted. Sprunt and Brace (1974) examined Westerly granite using SEM techniques, and estimated an aspect ratio distribution which showed a large number of cracks with aspect ratio greater than 10^{-2}. A similar, but more detailed, study by Hadley (1976) revealed a much larger proportion of aspect ratios on the order of 10^{-4} but also showed that the distribution depends on the stress history of the rock sample with prestressed samples containing a larger fraction of small aspect ratio cracks. Hadley (1976) concluded that a typical mean aspect ratio was of the order of 1×10^{-3}. Due to resolution limitations of the SEM technique, the smallest aspect ratio which was observable was estimated to be about 5×10^{-5}, but it is also clear that some limitations on the validity of the observations will result from the limited, two-dimensional sampling of three-dimensional cracks. Therefore, many small aspect ratio cracks in the rock could have been missed using the SEM imaging. Wong et al. (1989) also conclude that SEM images failed to detect a significant segment of the small aspect ratio population in a Westerly granite.

Direct observation of crack closure under uniaxial stress reveals other potential difficulties of the crack closure model used in this study. Batzle et al. (1980) showed that crack closure in Westerly granite can be incomplete due to the influence of roughness of the crack surfaces. In addition, the effects of crack intersections can be important in altering crack behavior as stress is applied. The crack roughness and intersections combined will clearly result in departures from the simple crack model locally, but it is not obvious how significant this effect will be on the macroscopic scale.

Other, indirect, investigations of crack dimensions have been conducted using differential strain analysis (DSA) techniques (Siegfried and Simmons, 1978). In principle, the DSA approach can produce information on crack aspect ratios by monitoring linear strain of a rock sample subjected to hydrostatic pressure. However, this method is subject to relatively large error due to numerical differentiation (Cheng and Toksöz, 1979). It is worth noting that Feves and Simmons (1976) found that the majority of cracks in a Westerly granite close at hydrostatic pressures of about 20 to 30 MPA, corresponding to an aspect ratio of about $5. \times 10^{-4}$ to 7.5×10^{-4} using the Walsh (1965) theory, a range which includes the results of our inversion. Cheng and Toksöz (1979) applied a velocity inversion technique for isotropic, hydrostatic pressure cases to Westerly granite and

find an aspect ratio distribution in general agreement with this result. It seems that our inversion results are corroborated by other indirect techniques using elastic properties in finding a significant amount of small aspect ratios for cracks within igneous rocks, while direct observations using SEM reveals porosity of larger aspect ratio. The larger aspect ratio porosity is a much less important source of variation in elastic behavior than the cracks under the pressure changes we consider here.

Permeability predictions

Permeability predictions using the qP and SH results from both aspect ratio distribution functions are shown in Figure 10, and they all compare favorably, though there is some variation for uniaxial stresses of 30 and 40 MPa. The curves for 10 MPa were normalized in the direction perpendicular to the applied stress to match a permeability measurement for Barre granite under 10 MPa hydrostatic pressure (Bernabé, 1986). This normalization assumes that the permeability in the direction perpendicular to the stress shows the same behavior as does isotropic permeability in the hydrostatic case. The other permeability curves were normalized to have the same permeability in the stress direction since the physical model for crack behavior includes no change in the crack distribution in this direction. In principle, the closure of cracks in other directions is also included in Eqs. (18) and (19), but the arbitrary normalization is still necessary. Without this scaling, the permeability predictions would actually rise in the stress direction as stress increases due to the lack of tortuosity effects in the permeability theory.

Laboratory experiments (Zoback and Byerlee, 1975) show that there is in fact a decrease in permeability in the direction parallel to the applied uniaxial stress, but this effect is not very large. Figure 11 compares the permeability measurements by Zoback and Byerlee (1975) to the constant values we would predict for permeability in the stress direction. The three data points in Figure 11 were measured by Zoback and Byerlee (1975) while increasing uniaxial stress on a sample of Westerly granite under 50 MPa confining pressure and 11 MPa pore pressure, and the curve between the two data is the trend inferred for permeability between these points. The Zoback and Byerlee (1975) data were made at very high uniaxial pressures to investigate dilatancy effects, and our theory is based on linear behavior which cannot be extrapolated to high stress.

While measurements of anisotropic permeability as a function of direction are not available to confirm the permeability predictions, the comparison to measurements parallel to the stress axis provide one check on the model, and a second check can be made by comparison with permeability measurements as a function of hydrostatic pressure. The permeability values perpendicular to the stress axis from both the qP and SH results are compared to the measurements by Bernabé (1986) for Barre granite in Figure 12. The predicted permeability decreases are too small, and, in addition, the measurements

show a tendency to decrease the most rapidly at the lower pressures, while the predictions have the opposite tendency. Within the limitations of the fact that we are comparing hydrostatic pressure and uniaxial stress cases, this suggests that some effects of crack closure are missing from our model. Other examples of permeability measurements reported in the literature for granites show a wide variation both in the absolute value of permeabilities under pressure and in the magnitude of change in isotropic permeability with increasing pressure (e.g., Brace et al. (1968) and Bernabé (1986)), so a perfect correlation would not necessarily be expected.

DISCUSSION AND CONCLUSIONS

The results of the velocity inversion suggest that the physical model for the fracture behavior under uniaxial stress is capable of describing most of the effects of the cracks on the elastic properties of the medium and that the model is able to match observations of velocity in the Barre granite. The aspect ratio of the dry fractures does not affect the elastic wave velocities in the Hudson formulation. Only the density of cracks ϵ is important in this case, and so the inversion results suggest that we are modeling this aspect of the system fairly well. On the other hand, permeability critically depends on the aspect ratio due to the cubic dependence on crack width in Eq. (14). The permeability predictions are highly sensitive to this parameter, and it is important to have an understanding of the aspect ratio distribution obtained by inversion.

Some insight into the roles of α_m and ϵ in the model of cracks and their effect on elastic behavior is obtained by independently inverting velocity data from different uniaxial stresses for crack density and α_m at each stress. Parameter results for the independent inversion procedure applied to the SH data are given in Table 4, and the theoretical velocities are compared to the data in Figure 13. Because α_m is allowed to vary at each stress, the velocity data are more accurately reproduced, though the joint inversion solutions are still preferred, since α_m should not be a function of pressure. Note that the velocity at 0 MPa is independent of aspect ratio and α_m cannot be determined for this case. The crack density values are almost identical to those obtained by the joint inversion (Table 2), but the results for α_m vary around the value 6.75×10^{-4}. Independent inversions of the qP data result in similar comparisons. From this and other properties of the inversion behavior, it is clear that the crack density is uniquely determined for each data set and serves to provide an overall shift upwards of the velocity curve as density reduces so that the mean velocity matches the mean of velocity observations. It can even be determined independently of the aspect ratio distribution. In contrast, the aspect ratio parameter α_m gives fine control of the shape of the velocity curve so that it may match the details of the data trends. It does this by governing the amount of fine cracks present for a given aspect ratio distribution which close at the pressure of interest.

Further understanding of the behavior of the inversion procedure is given by the similarity of the predictive capability of the flat and linear aspect ratio distributions in the velocity inversions (Figs. 4, 5, 6, 7, 8 and 9). This indicates a nonuniqueness of inversion results arising from the fact that enough cracks of aspect ratios which will close with the appropriate magnitudes of uniaxial stress are present in both distributions. Some constraints on this type of nonuniqueness can be made based on the accuracy of the velocity predictions resulting from the aspect ratio distributions. For example, an inversion based on a parabolic aspect ratio distribution proportional to $(\alpha - \alpha_m)^2$ was attempted. This parabolic distribution will have an even larger proportion of small aspect ratio cracks than the linear model in Eq. (7a). However, the inversion based on this distribution failed to converge to parameter values which could reproduce velocity data. This provides indirect evidence that the parabolic distribution is not realistic and that more larger aspect ratio cracks are required. On the other hand, the results of the two distributions presented above both reproduce data fairly well. Although the differences tend to be subtle in the plots of velocity predictions and data, the linear model is consistently somewhat better and also gives a smaller root mean square error, about 30% for the qP inversion and 17% for the SH case. This suggests that the linear model is in fact a better representation of the real crack distribution and that there are many fine cracks which cannot be resolved with SEM techniques. In addition, the larger value of maximum aspect ratio is encouraging since it is closer to the results of other studies (Feves and Simmons, 1976; Cheng and Toksöz, 1978), though in any case, the rock may contain porosity of even larger aspect ratio.

Nonuniqueness in the inversion also results from the assumption of noninteractive, penny-shaped cracks. Mavko and Nur (1978) consider a tapered crack model instead of ellipsoidal cracks and show that the two crack models can produce the same effects on elastic behavior, indicating an inherent lack of uniqueness. They also demonstrate that ellipsoidal crack models achieve these results with smaller values of aspect ratio. A theory accounting for the interactions of cracks will also give a larger estimate for aspect ratio than the noninteractive theories such as the Walsh (1965) model (Doyen, 1987). It is clear then that our results are dependent on the crack model, which assumes penny-shaped, noninteracting cracks. In summary, it seems that our results for crack density are well defined and reliable, but that the estimation of α_m must be considered more carefully in order to confirm its validity. This confirmation can be based on the accuracy of the inversion and on comparison to observation of aspect ratio distributions in rocks.

The ambiguity in the aspect ratio does not seem to have too large of an impact on permeability predictions, however (Figure 10). Instead, the dissimilarity between the hydrostatic data of Bernabé (1986) and the predictions for the direction perpendicular to the stress axis (Figure 12), is caused by other effects. There are two likely principal causes of this failure.

First, the permeability model fails to include the effects of interconnecting cracks. It is clear that intersections can affect crack closure (Batzle et al., 1980). Numerical studies in two-dimensional models of fractured materials show that connectivity is also very important for fluid flow (Long and Witherspoon, 1985). It is difficult to model these effects in the true three-dimensional medium. Snow (1969) presents an approach similar to our model of continuous planar fractures which is appropriate for several discrete sets of fractures but also neglects the effects of interconnection. Long et al. (1985) and Andersson and Dverstorp (1987) present numerical techniques for modeling the permeability of sets of penny-shaped cracks suspended in a three-dimensional volume. An application of our inversion technique could be to develop crack aspect ratio and orientation models for procedures like this.

A second source of error in our permeability calculations is that the present version of this theory does not include any change in aspect ratio for the cracks which remain open. In actuality, the aspect ratio of the open cracks will decrease as the uniaxial stress is applied (Toksöz et al., 1976). This effect will tend to decrease the permeability values in directions away from the stress axis. This is one major reason that permeability predictions for 10 MPa show an almost imperceptible drop from the constant 0 MPa case. The largest crack which will completely close in the Barre granite at this pressure, the crack with a normal parallel to the stress axis, has an aspect ratio 1.1×10^{-4}. With the cubic law behavior of the crack permeability, the cracks with aspect ratios smaller than this value have minimal contribution to fluid flow even in the zero stress case. The permeability prediction would drop further and be more realistic if the partial closure of cracks with initial aspect ratios larger than 1.1×10^{-4} was incorporated into the modeling scheme.

The change in aspect ratio with stress will affect only the permeability predictions as long as the cracks are dry. If, however, the cracks are assumed to be filled with a fluid, the aspect ratio also affects the elastic constant values. The forward modeling of velocities would then have to include the variation of aspect ratio with direction in order to compute the velocity values. However, a relatively small amount of gas mixed with the fluid will still cause the effective properties of the medium to be essentially that of a gas, since the effective bulk modulus k^* of a two phase medium is given by

$$(k^*)^{-1} = Vk_f^{-1} + (1 - V)k_g^{-1} \qquad (20)$$

where k_f and k_g are fluid and gas bulk moduli, respectively, and V is the volume fraction of fluid (Kuster and Toksöz, 1974). The large compressibility of the gas will tend to dominate the overall properties of the crack filling material, and it will tend to behave as though the cracks are filled with a gas. As long as the shear modulus and bulk modulus of the crack filling material are small, the aspect ratio of the cracks has little impact on the elastic constants in the Hudson (1981) approach, and the present approach will be sufficient.

This approach should at least provide a means of obtaining an initial estimate of permeabilities for use in modeling of fluid flow in subsurface fractured media. Potential areas of application include both hydrological studies and petroleum reservoir modeling. Perhaps the most important aspect of the theory is that it represents an attempt to extend knowledge of the permeability of a subsurface feature to regions beyond the borehole using seismic data.

ACKNOWLEDGEMENTS

REFERENCES

Andersson, J., and B. Dverstorp, Conditional simulations of fluid flow in three-dimensional networks of discrete fractures, *Water Resourc. Res.*, *23*, 1876–1886, 1987.

Batzle, M.L., G. Simmons, and R.W. Siegried, Microcrack closure in rocks under stress: direct observation, *J. Geophys. Res.*, *85*, 7072–7090, 1980.

Ben-Menahem, A., and S.J. Singh, *Seismic Waves and Sources*, Springer-Verlag, New York, 1981.

Bernabé, Y., Pore volume and transport properties changes during pressure cycling of several crystalline rocks, *Mech. Mater.*, *5*, 235–249, 1986.

Brace, W.F., J.B. Walsh, and W.T. Frangos, Permeability of granite under high pressure, *J. Geophys. Res*, *73*, 2225–2236, 1968.

Brown, S.R., Fluid flow through rock joints: the effect of surface roughness, *J. Geophys. Res.*, *92*, 1337–1347, 1987.

Cheng, C.H., and M.N. Toksöz, Inversion of seismic velocities for the pore aspect ratio spectrum of a rock, *J. Geophys. Res.*, *84*, 7533–7543.

Crampin, S., A review of the effects of anisotropic and cracked elastic-media., *Wave Motion*, *3*, 343-391, 1981.

Crampin, S., Effective anisotropic elastic constants for wave propagation through cracked solids, *Geophys. J. R. astr. Soc.*, *76*, 135–145, 1984.

Doyen, P.M., Crack geometry in igneous rocks: a maximum entropy inversion of elastic and transport properties, *J. Geophys. Res.*, *92*, 8169–8181, 1987.

Feves, M., and G. Simmons, Effects of stress on cracks in Westerly granite, *Bull. Seis. Soc. Amer.*, *66*, 1755–1765, 1976.

Hadley, K., 1976, Comparison of calculated and observed crack densities and seismic velocities in Westerly granite, *J. Geophys. Res.*, *81*, 3484–3494, 1976.

Hatton, L., M.H. Worthington, and J. Makin, *Seismic Data Processing*, Blackwell Scientific Publications, Oxford, 1986.

Hearmon, R.F.S., *An Introduction to Applied Anisotropic Elasticity*, Oxford, New York, 1961.

Hudson, J.A., Overall properties of a cracked solid, *Math. Proc. Camb. Phil. Soc.*, *88*, 371–384, 1980.

Hudson, J.A., Wave speeds and attenuation of elastic waves in material containing cracks, *Geophys. J. R. astr. Soc.*, *64*, 133–150, 1981.

Kuster, G.T. and M.N. Toksöz, Velocity and attenuation of seismic waves in two-phase media: Part I. Theoretical formulations, *Geophysics*, *39*, 607–618, 1974.

Lo, T.W., K.B. Coyner, and M.N. Toksöz, Experimental determination of elastic anisotropy of Berea sandstone, Chicopee shale, and Chelmsford granite, *Geophys.*, *51*, 164–171, 1986.

Long, J.C.S., and P.A. Witherspoon, The relationship of the degree of interconnection to permeability in fracture networks, *J. Geophys. Res.*, *90*, 3087–3098, 1985.

Long, J.C.S., P. Gilmour, and P.A. Witherspoon, A model for steady fluid flow in three-dimensional networks of disc-shaped fractures, *Water Resourc. Res.*, *21*, 1105-1115, 1985.

Mavko, G.M., and A. Nur, The effect of nonelliptical cracks on the compressibility of rocks, *J. Geophys. Res.*, *83*, 4459–4468, 1978.

Morris, P.R., Averaging fourth-rank tensors with weight functions, *J. Appl. Phys.*, *40*, 447–448, 1969.

Musgrave, M.P.J., *Crystal Acoustics*, Holden-Day, San Francisco, 1970.

Nur, A., Effects of stress on velocity anisotropy in rocks with cracks, *J. Geophys. Res.*, *76*, 2022–2034, 1971.

Nur, A., and G. Simmons, Stress-induced velocity anisotropy in rock: an experimental study, *J. Geophys. Res.*, *27*, 6667–6674, 1969.

Sayers, C.M., Angular dependent ultrasonic wave velocities in aggregates of hexagonal crystals, *Ultrasonics*, *24*, 289–291, 1986.

Sayers, C.M., Inversion of ultrasonic wave velocity measurements to obtain the microcrack orientation distribution function in rocks, *Ultrasonics*, *26*, 73–77, 1988a.

Sayers, C.M., Stress-induced ultrasonic wave velocity anisotropy in fractured rock, *Ultrasonics*, *26*, 311–317, 1988b.

Siegfried, R., and G. Simmons, Characterization of oriented cracks with differential strain analysis, *J. Geophys. Res.*, *83*, 1269–1278, 1978.

Snow, D.T., Anisotropic permeability of fractured media, *Water Resourc. Res.*, *5*, 1273–1289, 1969.

Sprunt, E., and W.F. Brace, Direct observation of microcavities in crystalline rocks, *Int. J. Rock Mech. Mining Sci.*, *11*, 139–150, 1974.

Tarantola, A., *Inverse Problem Theory*, Elsevier, Amsterdam, 1987.

Toksöz, M.N., C.H. Cheng, and A. Timur, Velocities of seismic waves in porous rocks, *Geophysics*, *41*, 621–645, 1976.

Tsang, Y.W., and P.A. Witherspoon, Hydromechanical behavior of a deformable rock fracture subject to normal stress, *J. Geophys. Res.*, *86*, 9287–9298, 1981.

Tsang, Y.W., and P.A. Witherspoon, The dependence of fracture mechanical and fluid flow properties on fracture roughness and sample size, *J. Geophys. Res.*, *88*, 2359–2366, 1983.

Walsh, J.B., The effects of cracks on the uniaxial elastic compression of rocks, *J. Geophys. Res.*, *70*, 399–411, 1965.

Wong, T.-F., J.T. Fredrich, and G.D. Gwanmesia, Crack aperture statistics and pore space fractal geometry of Westerly granite and Rutland quartzite: implications for an elastic contact model of rock compressibility, *J. Geophys. Res.*, *94*, 10267–10278, 1989.

Zoback, M.D., and J.D. Byerlee, The effect of microcrack dilatancy on the permeability of Westerly granite, *J. Geophys. Res.*, *80*, 752–755, 1975.

	Aspect Ratio Distribution Function	
Parameter	Flat	Linear
α_m	3.99×10^{-4}	6.34×10^{-4}
ϵ_0	0.275	0.275
ϵ_{10}	0.253	0.254
ϵ_{20}	0.235	0.235
ϵ_{30}	0.221	0.221

Table I. Inversion results using qP velocity measurements of Nur and Simmons (1969). The subscript P on ϵ_P indicates the uniaxial stress value for each crack density.

	Aspect Ratio Distribution Function	
Parameter	Flat	Linear
α_m	4.48×10^{-4}	6.75×10^{-4}
ϵ_0	0.315	0.315
ϵ_{10}	0.286	0.285
ϵ_{20}	0.257	0.256
ϵ_{30}	0.235	0.234
ϵ_{40}	0.214	0.215

Table 2. Inversion results using SH velocity measurements of Nur and Simmons (1969). The subscript P on ϵ_P indicates the uniaxial stress value for each crack density.

Gibson and Toksöz

Parameter	Aspect Ratio Distribution Function	
	Flat	Linear
α_m	7.34×10^{-4}	13.1×10^{-4}
ϵ_0	0.314	0.314
ϵ_{10}	0.286	0.285
ϵ_{20}	0.252	0.252
ϵ_{30}	0.227	0.227
ϵ_{40}	0.206	0.206

Table 3. Inversion results using qSV velocity measurements of Nur and Simmons (1969). The subscript P on ϵ_P indicates the uniaxial stress value for each crack density.

Uniaxial stress (MPa)	ϵ	α_m
0	0.315	
10	0.283	4.98×10^{-4}
20	0.255	5.94×10^{-4}
30	0.234	6.78×10^{-4}
40	0.217	5.61×10^{-4}

Table 4. Results of independent inversion of SH velocity measurements [Nur and Simmons, 1969) for crack density ϵ and maximum aspect ratio α_m at each stress. The inversion cannot determine information on aspect ratio at 0 MPa.

P = 0

P>0
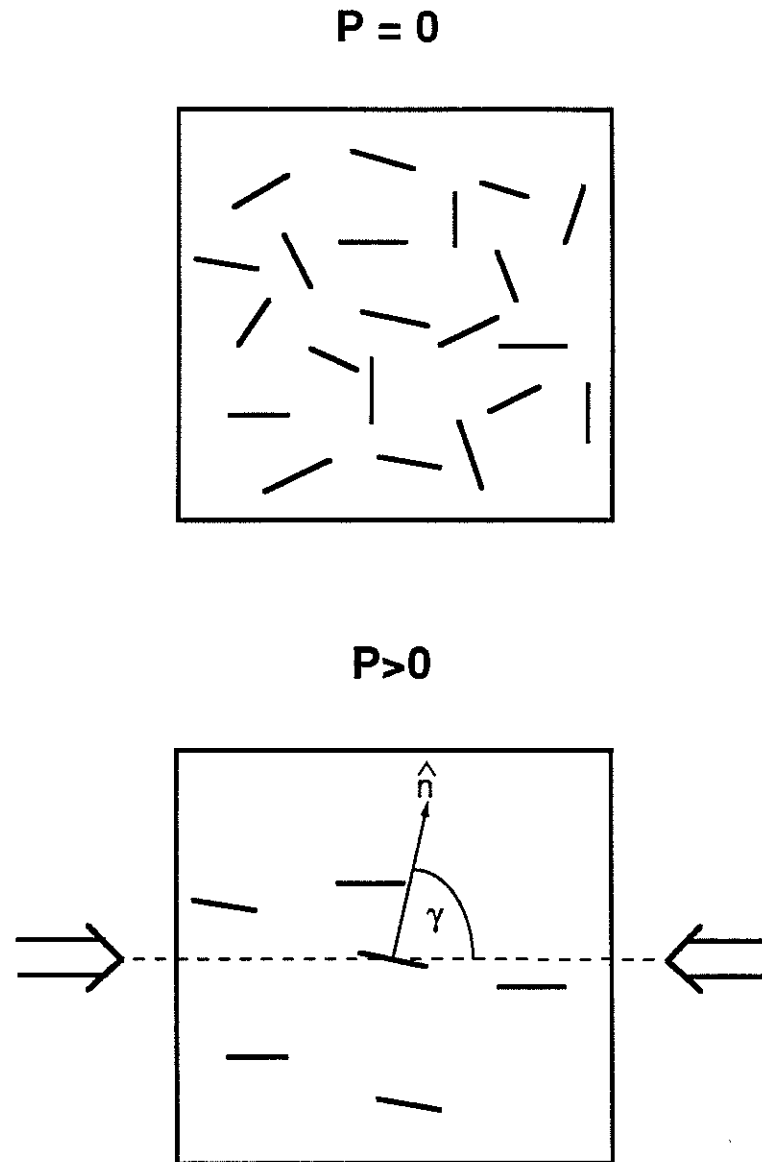
Figure 1: Schematic diagram illustrating the behavior of a randomly fractured medium under an applied uniaxial stress. The upper figure shows a possible random crack system with no stress applied. The lower portion shows the same system after application of the uniaxial stress, where cracks have closed depending on their orientation with respect to the stress. If the angle γ indicated on the figure is equal to or smaller than the angle γ_0 defined in the text, the crack will close under the applied uniaxial stress.
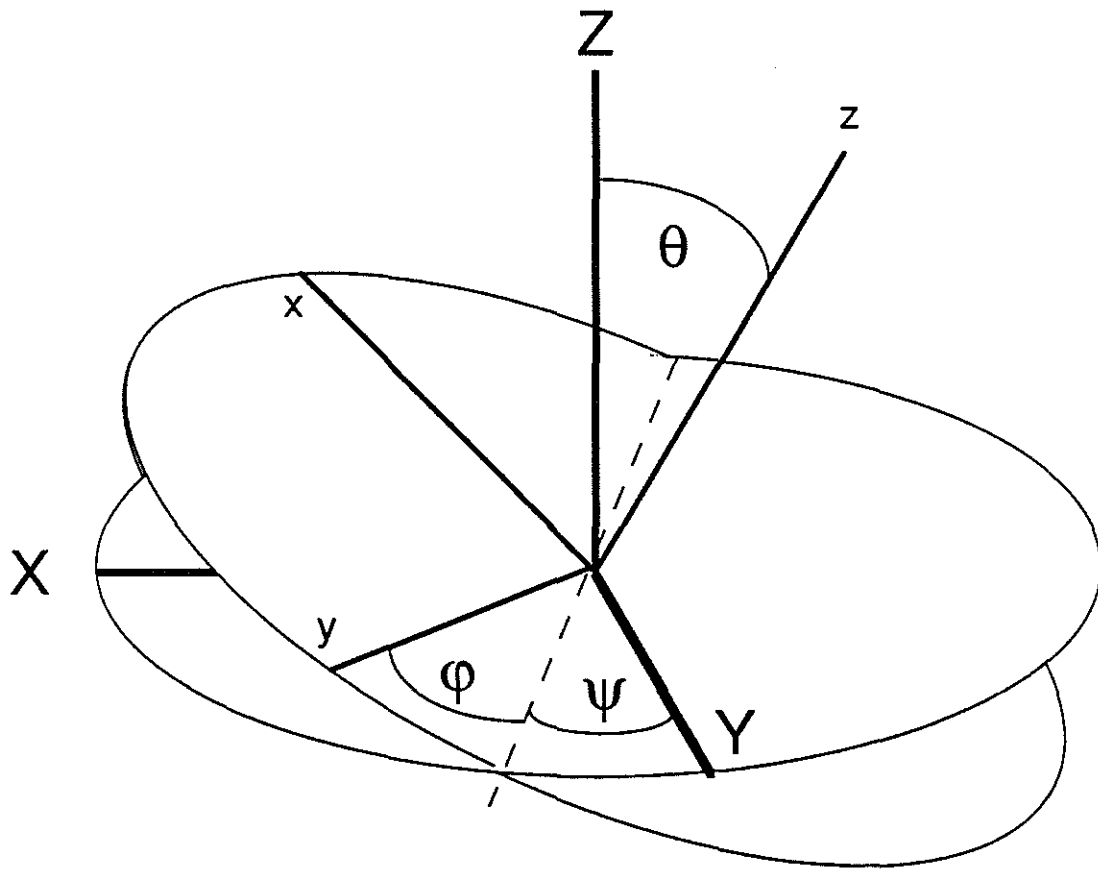
Figure 2: Euler angles of rotation θ, ψ, ϕ describing orientation of a given crack coordinate system x, y, z (fine lines) with respect to the composite medium coordinate system X, Y, Z (heavy lines). The dashed line indicates the intermediate position of the y axis, and the two disks represent the $X - Y$ planes before and after rotation, which are also the crack planes. The set of rotations is defined as follows: 1) rotate by ψ about Z (the same as z initially). 2) rotate by θ about the new y-axis. 3) rotate by ϕ about the new z-axis. Since the cracks are assumed to have circular symmetry, the first two rotations actually uniquely specify the orientation of a single crack.
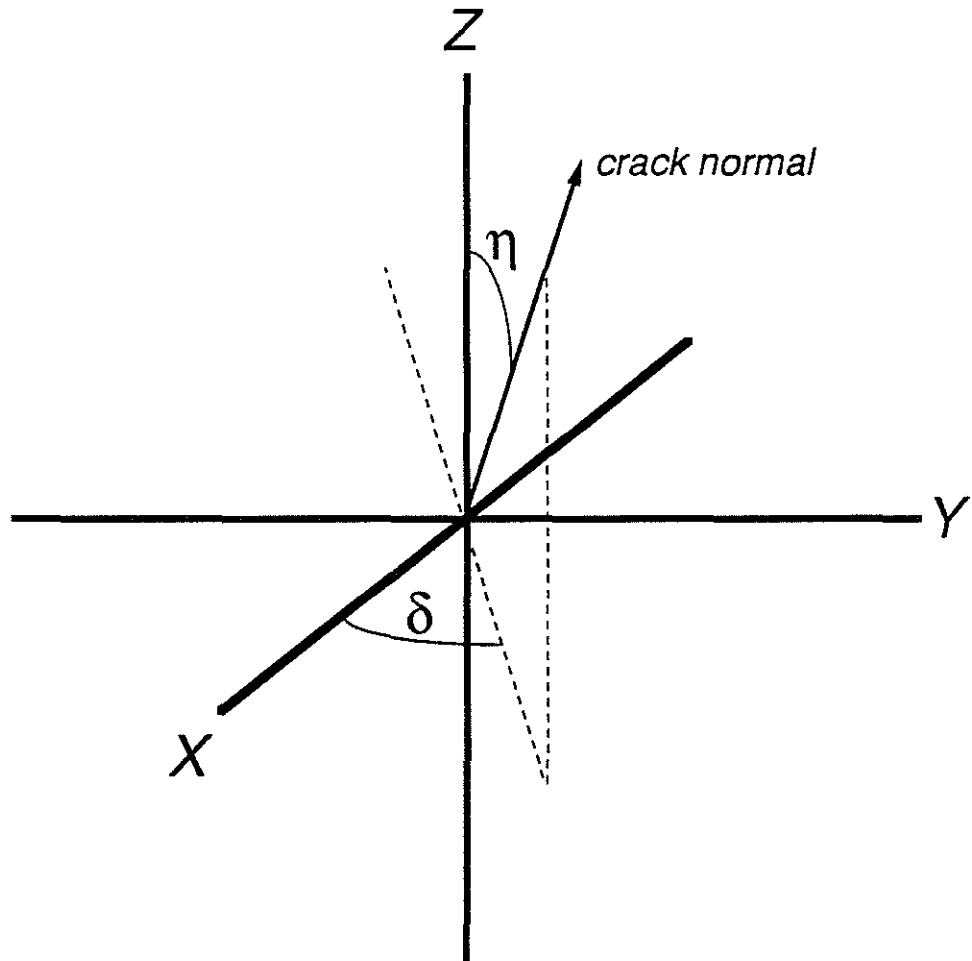
Figure 3: The angles δ and η necessary to specify the orientation of a crack normal.
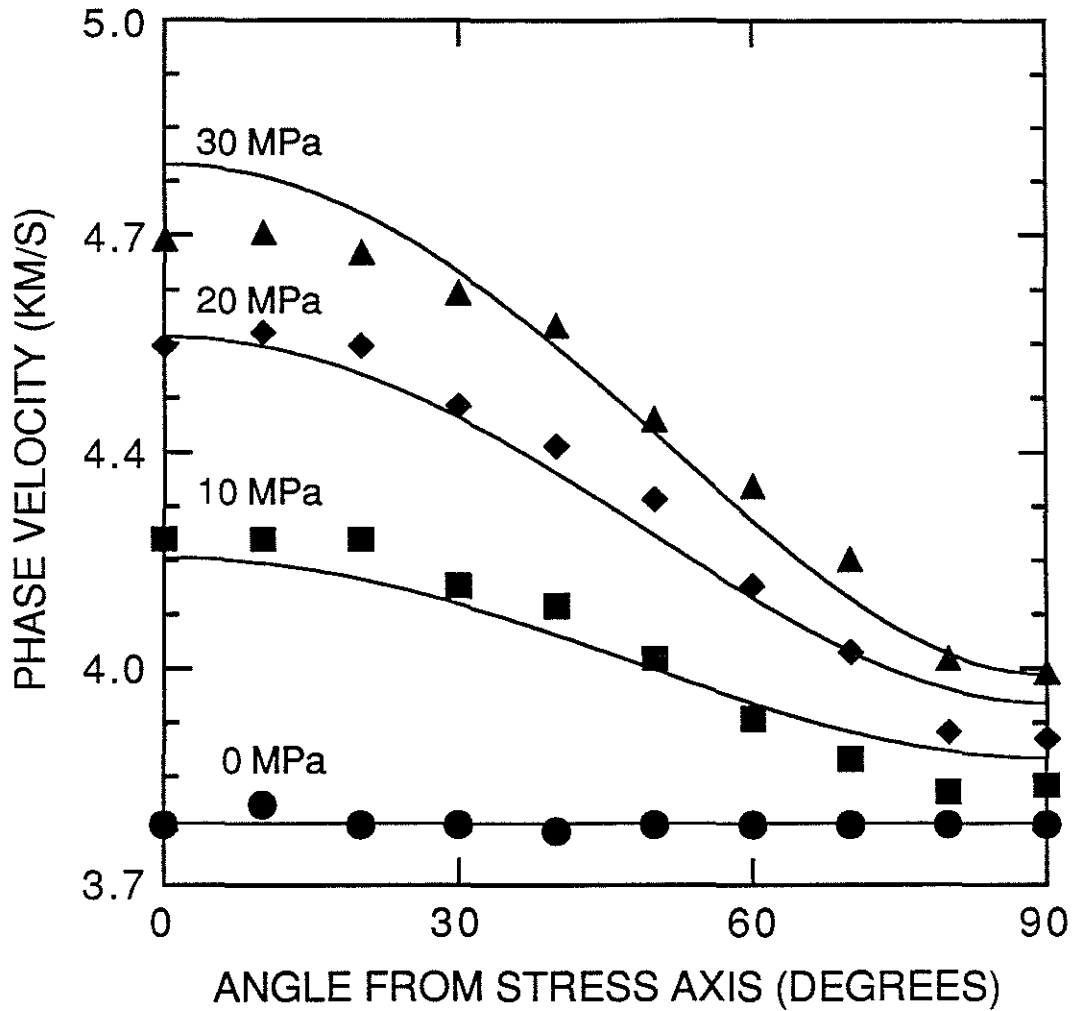
Figure 4: Results of inversion for crack density ϵ and maximum aspect ratio α_m using
Barre granite quasi-compressional wave velocity data and the linear aspect ratio
distribution function (Eq. (7a)). The points are data collected by Nur and Sim-
mons (1969), and the lines indicate the results of a joint inversion of all of the data
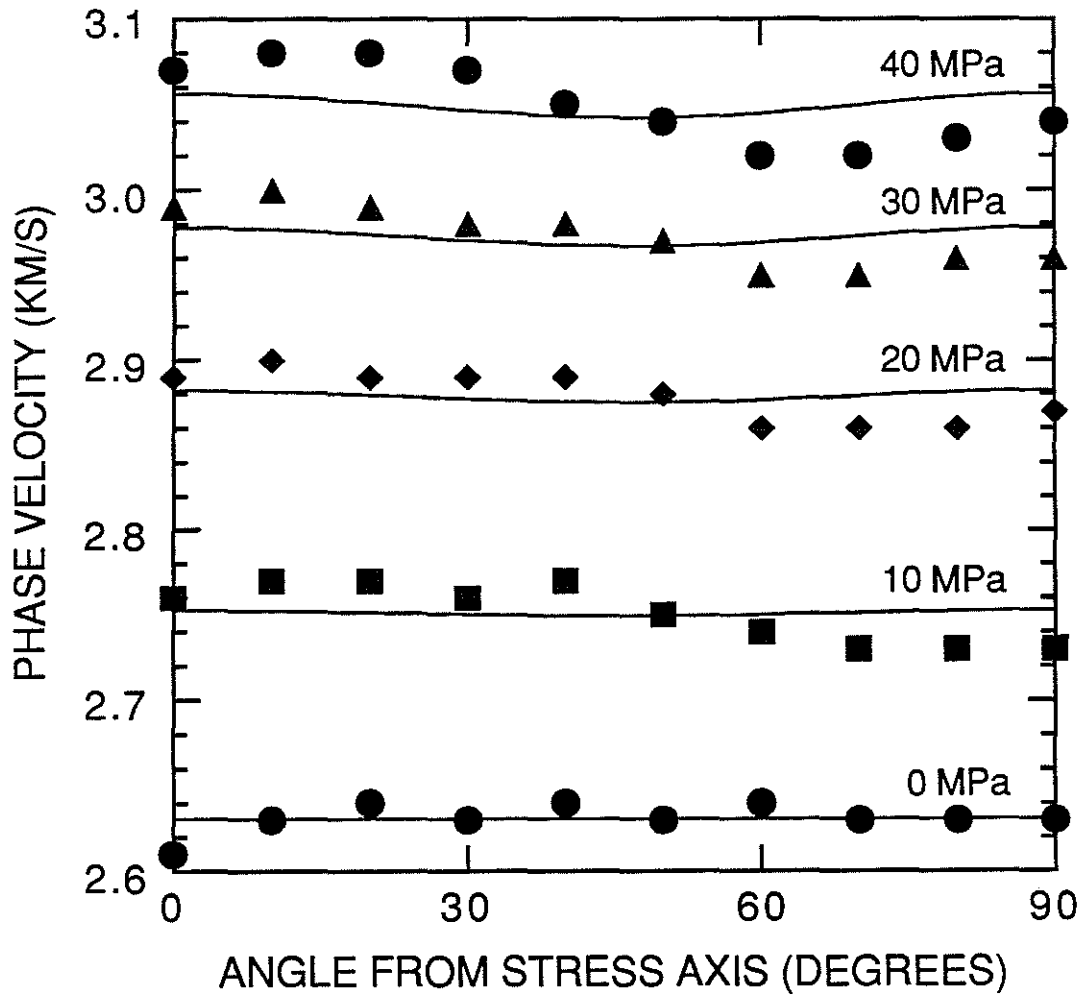in this figure. The value of the applied uniaxial stress is indicated for each curve.
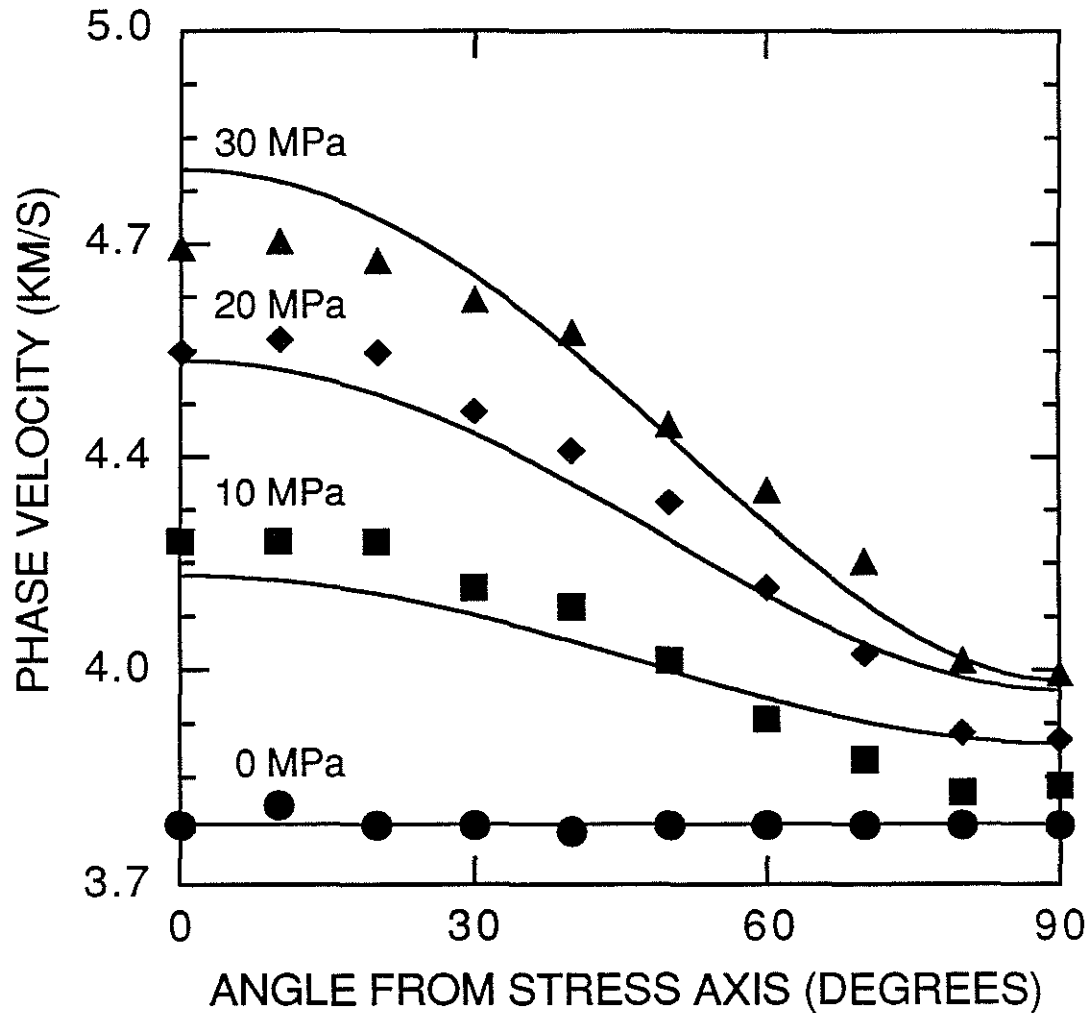
Figure 5: Results of inversion for crack density ϵ and maximum aspect ratio α_m using Barre granite quasi-compressional wave velocity data and the flat aspect ratio distribution function (Eq. (7b)). The points are data collected by Nur and Simmons (1969), and the lines indicate the results of a joint inversion of all of the data in this figure. The value of the applied uniaxial stress is indicated for each curve.
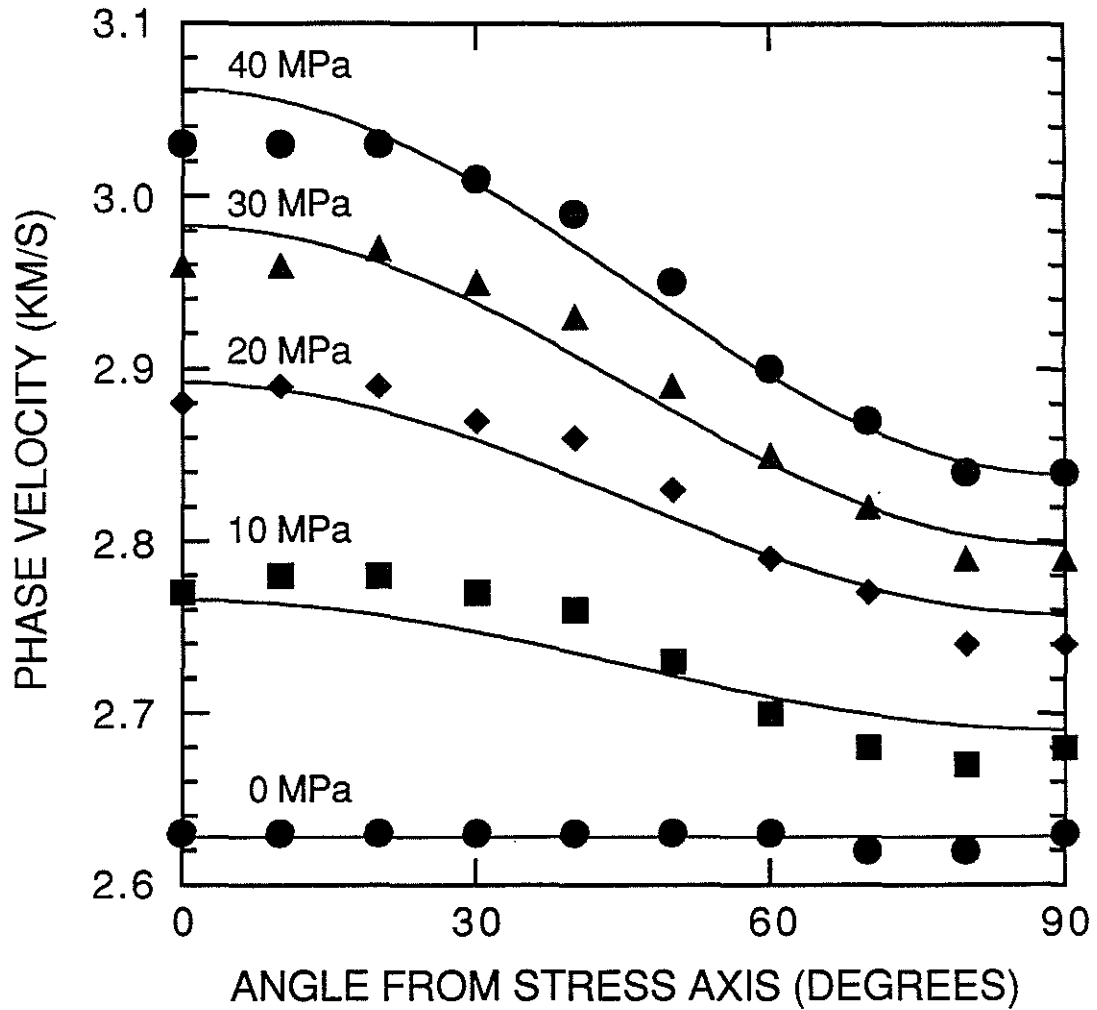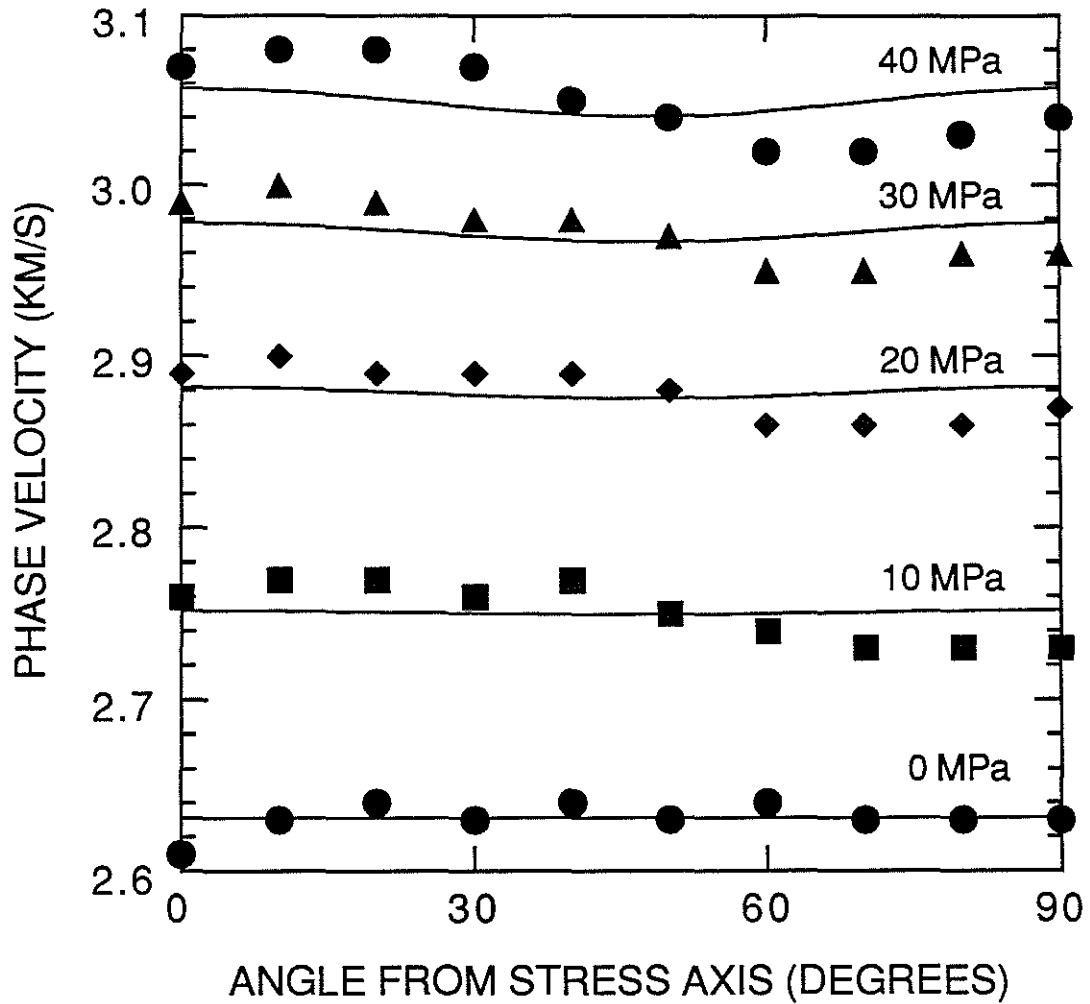
Figure 6: Results of inversion for crack density ϵ and maximum aspect ratio α_m using Barre granite SH velocity data and the linear aspect ratio distribution (Eq. (7a)). The points are data collected by Nur and Simmons (1969), and the lines indicate the results of a joint inversion of all of the data in this figure. The value of the applied uniaxial stress is indicated for each curve.
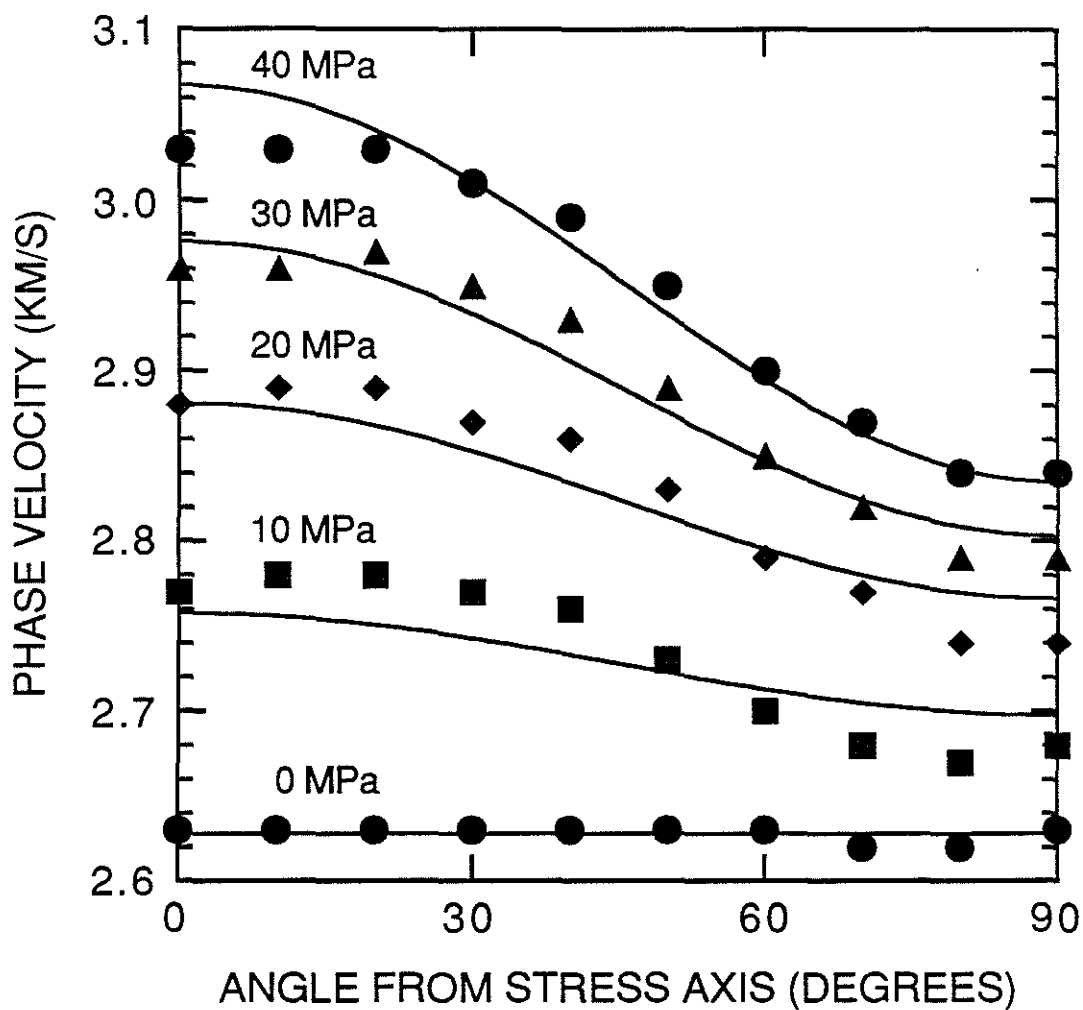
Figure 7: Results of inversion for crack density ϵ and maximum aspect ratio α_m using Barre granite SH velocity data and the flat aspect ratio distribution (Eq. (7b)). The points are data collected by Nur and Simmons (1969), and the lines indicate the results of a joint inversion of all of the data in this figure. The value of the applied uniaxial stress is indicated for each curve.

Figure 8: Results of inversion for crack density ϵ and maximum aspect ratio α_m using Barre granite qSV velocity data and the linear aspect ratio distribution (Eq. (7a)). The points are data collected by Nur and Simmons (1969), and the lines indicate the results of a joint inversion of all of the data in this figure. The value of the applied uniaxial stress is indicated for each curve.

Figure 9: Results of inversion for crack density ϵ and maximum crack size α_m using Barre granite qSV velocity data and the flat aspect ratio distribution (Eq. (7b)). The points are data collected by Nur and Simmons (1969), and the lines indicate the results of a joint inversion of all of the data in this figure. The value of the applied uniaxial stress is indicated for each curve.
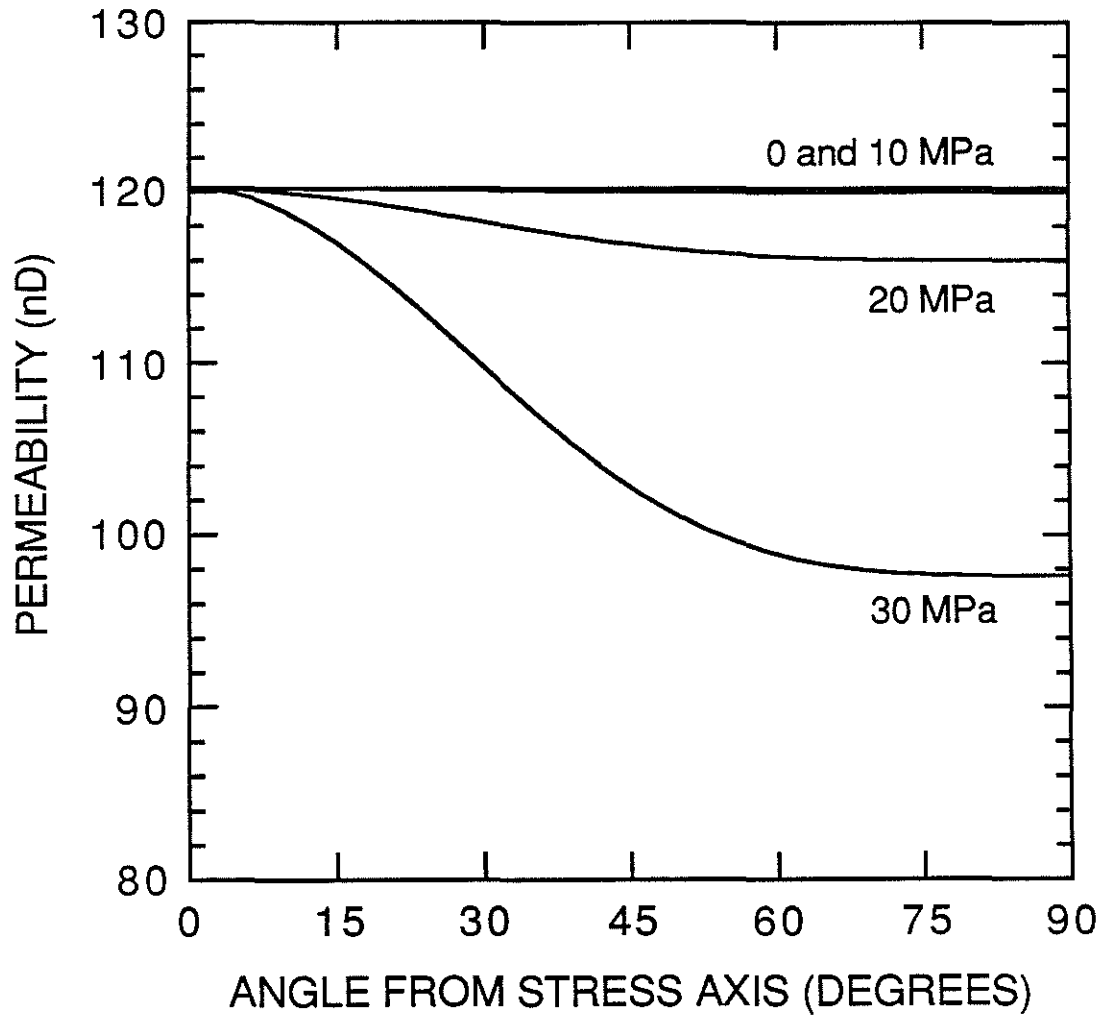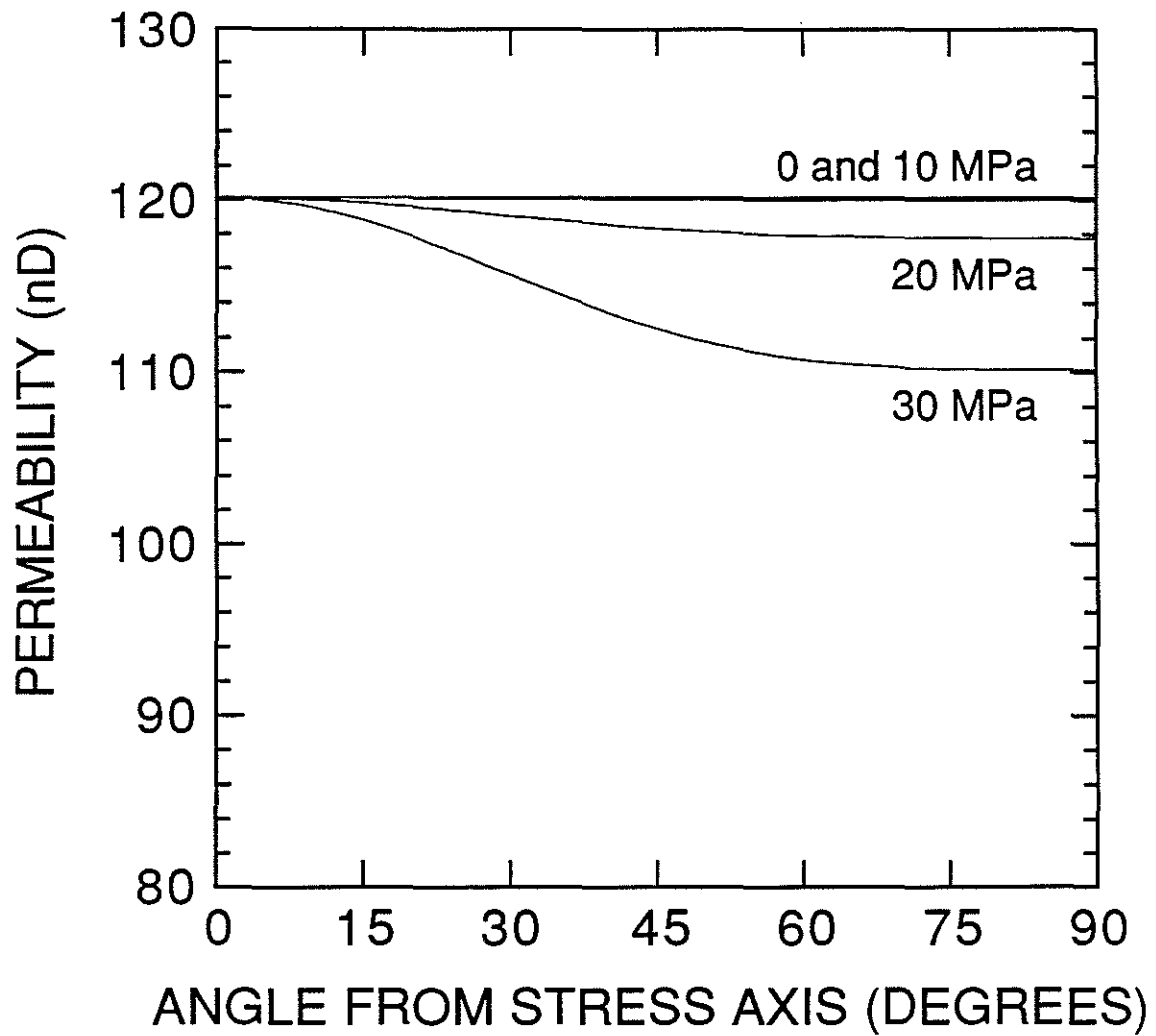
Figure 10: a) Permeability predictions as a function of angle from the applied uniaxial
stress axis. The predictions use the results from the inversion of qP data and the
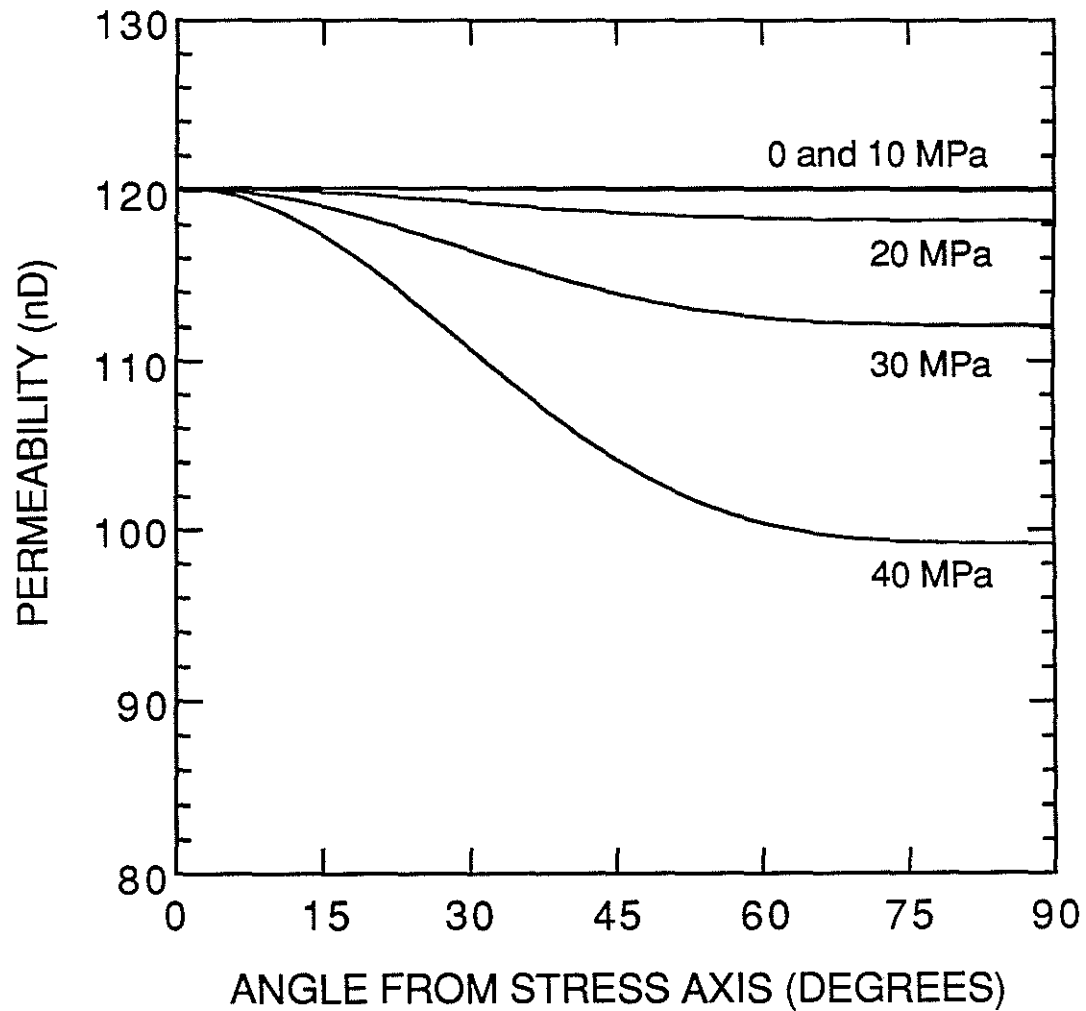flat aspect ratio distribution. The uniaxial stress is indicated for each curve.
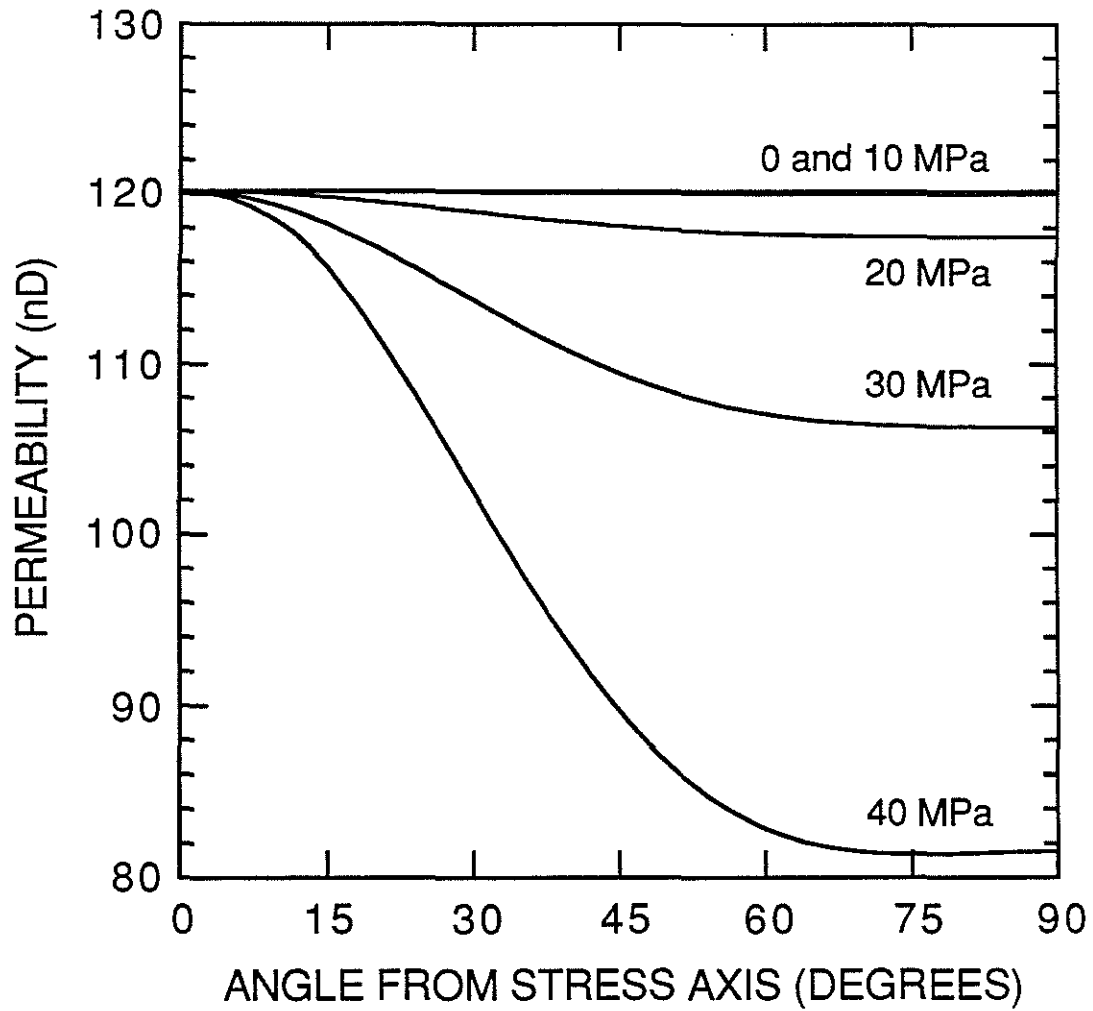
Figure 10: b) Permeability predictions as a function of angle from the applied uniaxial
stress axis. The predictions use the results from the inversion of SH data and the
flat aspect ratio distribution. The uniaxial stress is indicated for each curve.

Figure 10: c) Permeability predictions as a function of angle from the applied uniaxial stress axis. The predictions use the results from the inversion of qP data and the linear aspect ratio distribution. The uniaxial stress is indicated for each curve.

Figure 10: d) Permeability predictions as a function of angle from the applied uniaxial stress axis. The predictions use the results from the inversion of SH data and the linear aspect ratio distribution. The uniaxial stress is indicated for each curve.
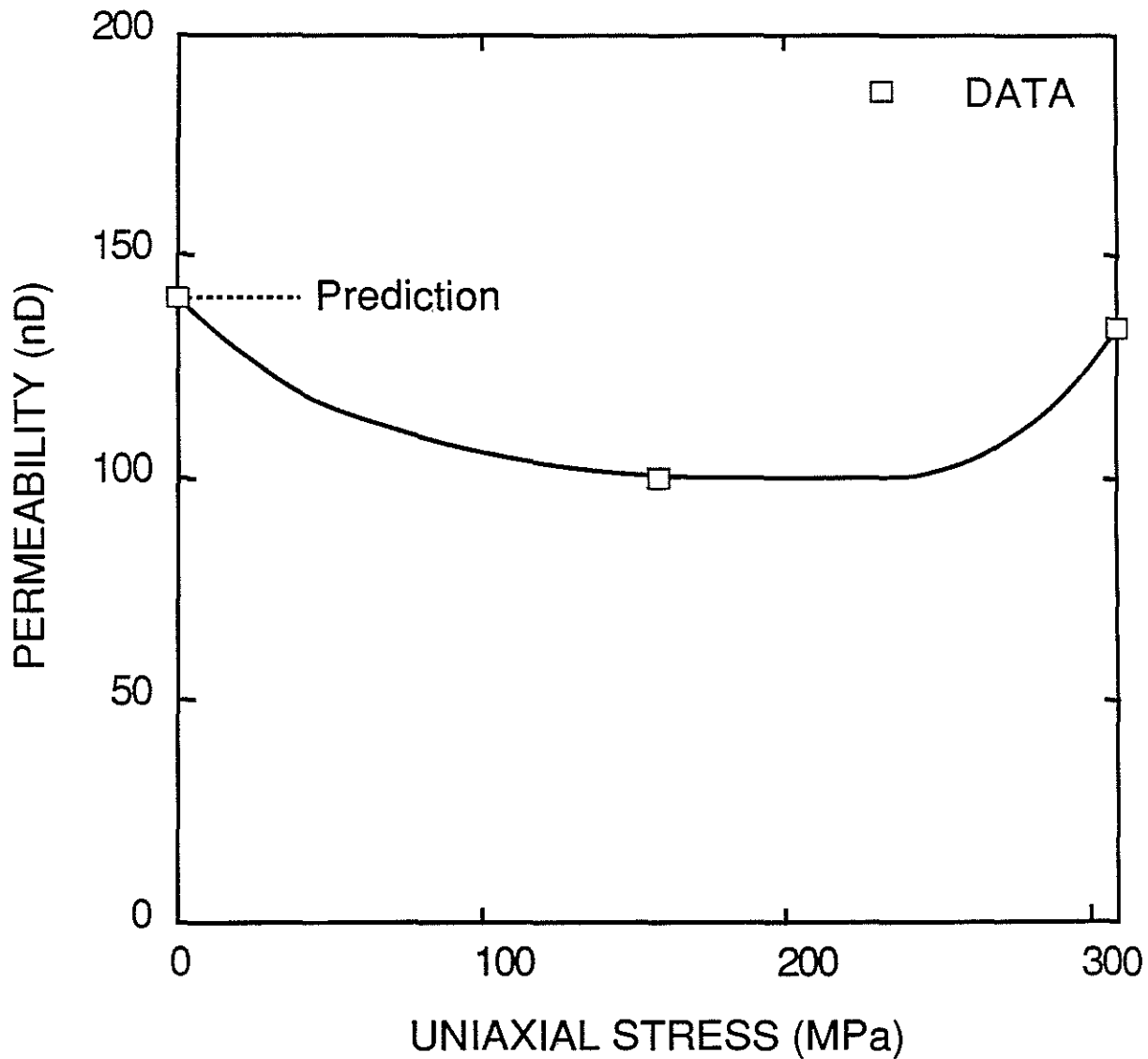
Gibson and Toksöz

Figure 11: Comparison of permeability predictions parallel to the stress axis with measurements by Zoback and Byerlee (1975) of permeability parallel to the stress axis in an experiment performed on Westerly granite. The curve inferred by Zoback and Byerlee (1975) to represent permeability behavior between data points at 0 MPa and 310 MPa is given by the solid line. The constant permeability which would be predicted by the theoretical model over the pressure range investigated by Nur and Simmons (1969) is indicated.
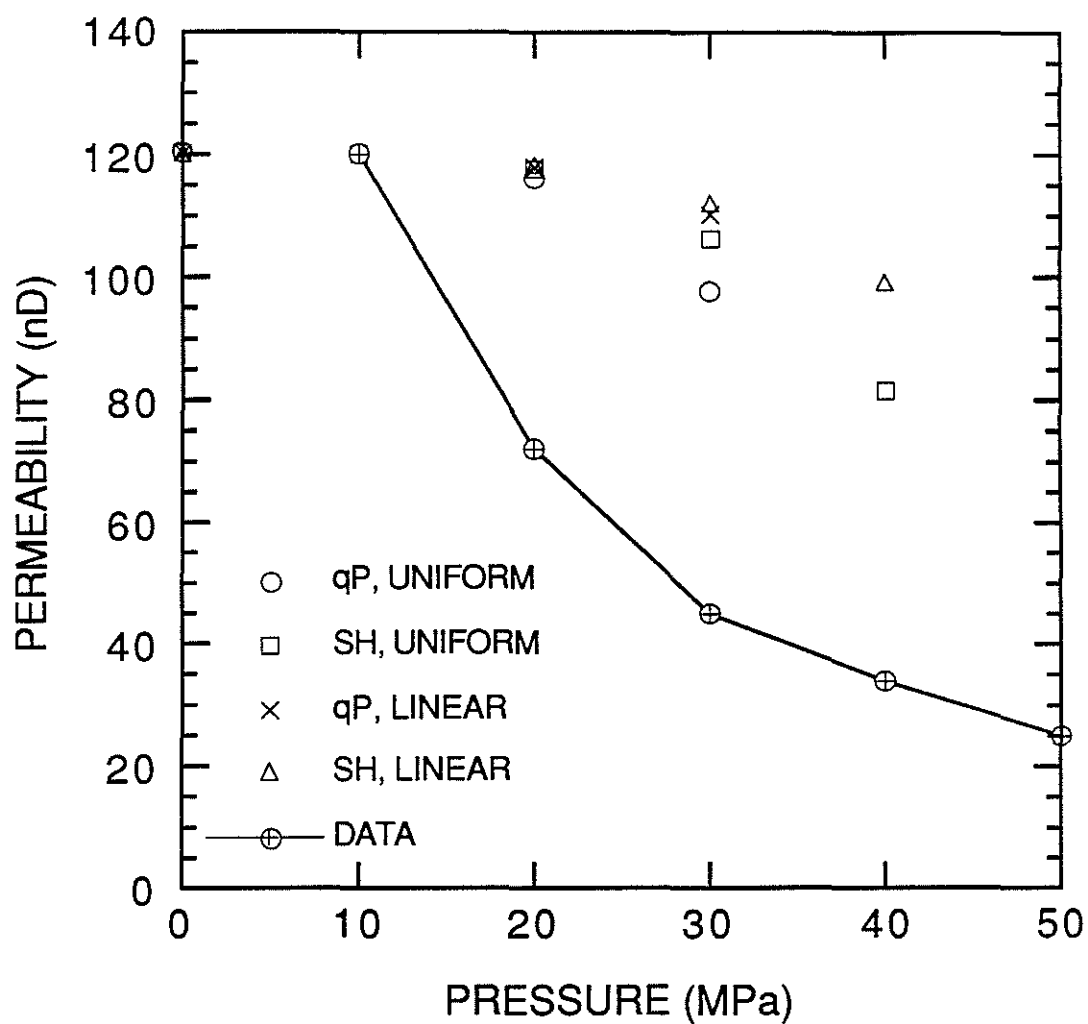
Figure 12: Comparison of hydrostatic permeability measurements with theoretical permeabilities perpendicular to the stress axis. The data, measurements on Barre granite (Bernabé, 1986), are indicated by the line and the points are calculated from Eqs. (18) and (19). Since the permeabilities are normalized to have the same value at 10 MPa, the data and theoretical points overlap at this value of stress. The velocity data types used to calculate the permeability predictions are indicated in the figure.
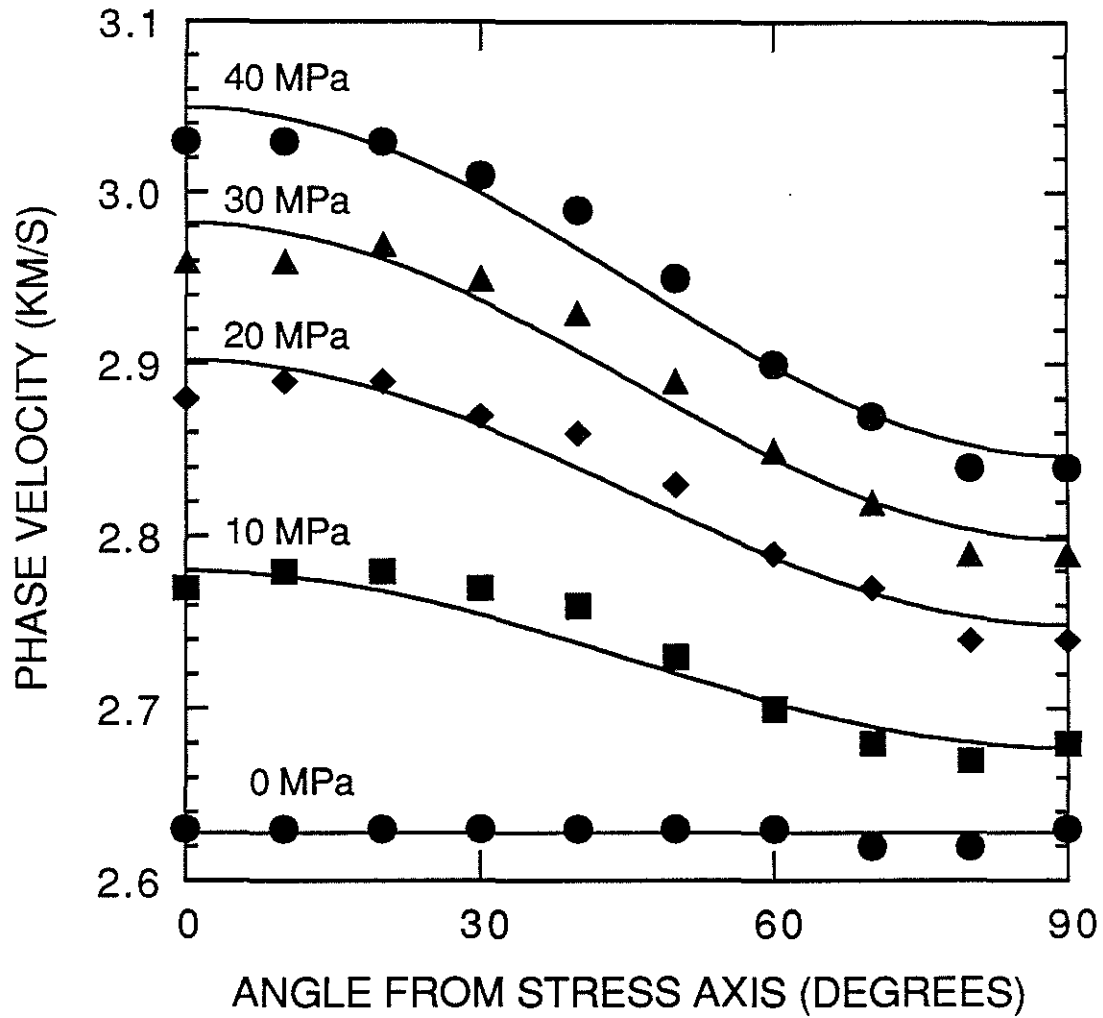
Figure 13: Results of independent inversions for crack density ϵ and maximum crack size α_m of Barre granite SH velocity data. The points are data collected by Nur and Simmons (1969), and the lines indicate the inversion results. The value of the applied uniaxial stress is indicated for each curve.